Journal of Petroleum Science and Engineering 212 (2022) 110248

Contents lists available at ScienceDirect

Journal of Petroleum Science and Engineering

journal homepage: www.elsevier.com/locate/petrol

Siderite occurrence in petroleum systems and its potential as a hydrocarbon-migration proxy: A case study of the Catcher Area Development and the Bittern area, UK North Sea

Maryam A. Abdulkarim [a,b,*], Adrian R. Muxworthy [a], Alastair Fraser [a], Martin Neumaier [a], Pengxiang Hu [c], Alison Cowan [a]

[a] Department of Earth Science and Engineering, Imperial College, London, SW7 2AZ, UK
[b] Department of Petroleum Engineering, Baze University, Abuja, Nigeria
[c] Research School of Earth Sciences, Australian National University, Canberra, 2601, Australia

ARTICLE INFO

Keywords:
Mineral magnetism
Siderite in hydrocarbon reservoirs
Hydrocarbon migration
Magnetic susceptibility
Diagenesis
UK Central North Sea

ABSTRACT

We report a detailed magnetic study of Tertiary sandstone cores from the Bittern field, West Central Graben, and Catcher Area Development (CAD), West Central Shelf, UK North Sea that identified siderite as a potential magnetic proxy for the differentiation of vertical and lateral hydrocarbon migration. Magnetic hysteresis experiments revealed increased presence of paramagnetic minerals in the oil-stained sandstones of the fields compared to the nearby dry Tertiary (unstained) sandstone of offset wells. Within the oil-stained sandstones, the paramagnetic proportion is highly variant, with low and high paramagnetic sections present. Detailed experiments including thermomagnetometry between 10 K and 900 K and XRD analysis, combined with Mössbauer spectroscopy confirmed that this increase in paramagnetic response was primarily due to the formation of siderite. An increase in the quantity of paramagnetic clays and occasionally pyrite also contributed to the increased response. Siderite and iron sulphides have been interpreted to form during hydrocarbon migration and potentially oil biodegradation. We propose that hydrocarbon migration pathways may be indicated by the distribution of siderite. We argue that as hydrocarbons migrate vertically and the equilibrium partial pressure of CO_2 with the environment reduces, essential HCO_3^- is produced which reacts with available Fe^{2+} to form siderite if all the other diagenetic requirements for its formation are met. The distribution of siderite and magnetic susceptibility values along the oil-stained layer provides a tool for the determination of the migration pathways in low sulphur hydrocarbon environments containing reactive iron.

1. Introduction

It is well-established that hydrocarbons have the potential to alter the magnetic mineralogy of sedimentary rocks leading to either a magnetic enhancement or reduction (e.g Costanzo-Alvarez et al., 2006; Emmerton et al., 2013; Machel, 1995). Recent studies have shown the potential of mineral magnetic methods to determine hydrocarbon migration pathways (Abubakar et al., 2020; Badejo et al., 2021c); this finding could potentially be applied in petroleum exploration and development in near-mature and potentially frontier hydrocarbon basins. Abubakar et al. (2020) and Badejo et al. (2021a, 2021b, 2021c) suggest the presence of different magnetic minerals along migration pathways, in particular, the presence of siderite. Badejo et al. (2021a, 2021b, 2021c) identified significant amount of siderite in oil field sandstones from the Central North Sea, UK, that were filled via vertical migration, but siderite was not present where lateral migration is thought to dominate. Abubakar et al. (2020) did not identify siderite in the Wessex Basin, UK, and petroleum systems modelling suggested mainly lateral migration in the area considered. This raises the questions; can siderite be used as a proxy for vertical migration? Is their finding universal or specific to certain environments? What is/are the mechanism(s) responsible for this differentiation? It is the aim of this study to answer these questions.

Siderite is a common authigenic cement found in sedimentary rocks and its formation is usually attributed to shallow (centimetre to a few hundreds of metres) sub-surface processes occurring during rock

* Corresponding author. Department of Earth Science and Engineering, Imperial College, London, SW7 2AZ, UK.
E-mail address: m.abdulkarim18@imperial.ac.uk (M.A. Abdulkarim).

https://doi.org/10.1016/j.petrol.2022.110248
Received 4 October 2021; Received in revised form 20 December 2021; Accepted 29 January 2022
Available online 1 February 2022

diagenesis (Liu et al., 1997; Larrasoaña et al., 2007; Lin et al., 2020). However, it is thought to also form at greater depths. Machel and Burton (1991) and Machel (1995) showed that the formation of siderite at depths of between 1 km and 6 km is thermodynamically likely if suitable diagenetic conditions are met, which include proximity to migrating and/or in-situ hydrocarbons. Rossi et al. (2001) identified siderite zonation in the Khatatba reservoirs in Egypt; they suggested that the precipitation of siderite took place at a period when the sediment was at least 3 km deep, probably after oil migration into the reservoir. Emmerton (2013) identified siderite at depths of between 2.5 and 3 km in oil-stained samples from the Brent Field, North Sea, whereas siderite was absent from nearby dry-well samples.

To investigate the potential of siderite as a magnetic proxy for hydrocarbon migration direction in oil and gas exploration, we carried out detailed magnetic studies on core samples from the Bittern oilfield and oilfields from Catcher Area Development (CAD) of the UK Central North Sea (Fig. 1 and Table 1). Apart from the significant amount of information available from seismic, well and core data which are accessible, the Bittern and the CAD fields were also selected due to the low degree of uncertainty with regards to the likely migration pathway of hydrocarbon into the reservoir (Robertson et al., 2013).

2. Study area

The Catcher Area Development (CAD) is located about 180 km ESE of Aberdeen and is a multiple field development consisting of six hydrocarbon fields (first discovery made in 2010) in the West Central Shelf of the UK North Sea (Table 1). The six oilfields are closely spaced, with a distance between individual fields of 2–5 km (Fig. 1). These reservoirs have excellent properties with porosity and permeability values of between 25% and 36%, and 1 Darcy and 5 Darcies respectively (Table 1). The CAD reservoirs comprise the Tay sandstone of the Horda formation and the Cromarty sands of the Upper Sele formation (Fig. 2) (Roberts et al., 2017) and the field complex is estimated to contain over 170 million barrels (MMbbls) of oil equivalent. The reservoirs are located at depths of between 1000 m and 1500 m True Vertical Depth Sub Sea (TVDSS). Geochemical analysis reveals that the oils in these reservoirs shows progressive degradation with decreasing depth and temperature (Forsythe et al., 2017a, 2017b).

The Bittern field, located about 200 km east of Aberdeen, was discovered in 1996 within block 29/1 of the West Central Graben, UK Central North Sea (Mccormick and Leishman, 2004). Its reservoir crest is located at approximately 2020 m below sea level and a water depth of approximately 93 m. Its anticlinal trapping system was obscured by a gas chimney present in shallower claystone formation between 910 and 1610 m. Consequently, earlier exploration did not consider it as an oil prospect (Mccormick and Leishman, 2004). The Cromarty and Forties sandstone makes up the productive section of the field (Fig. 2). Pressure analysis has suggested connectivity and fluid movement along the Cromarty sands of the Bittern and CAD fields (Robertson et al., 2013). The Bittern field is significant with original oil-in-place (OOIP) and original gas in place of 250 MMbbls and 300 billion cubic feet (BCF) respectively (Ritchie et al., 2011). The reservoir has an estimated porosity and permeability of 33% and 1D respectively, and net to gross of about 95%. The oil in place is a low sulphur high quality crude with density averaging at 39°API. Geochemical analysis on the produced hydrocarbons reveals no evidence of biodegradation.

2.1. Stratigraphic and sedimentological framework

The Central North Sea forms the southern arm of a trilete Jurassic rift system that defines the structure of the UK Northern North Sea Basin (Fraser et al., 2003). The rift formed by extension in the Late Jurassic which caused a significant deepening in water depths, basin isolation and the deposition of Upper Jurassic source rocks. Subsequent thermal subsidence through the Cretaceous and Tertiary resulted in the accumulation of over 5 kms of post rift sediments. Following a relatively quiescent period of mainly chalk and mudstone deposition in the Cretaceous, the initiation of the Iceland hotspot at ~60 Ma to the west of the UK led to massive uplift of the northern UK and the shedding of large

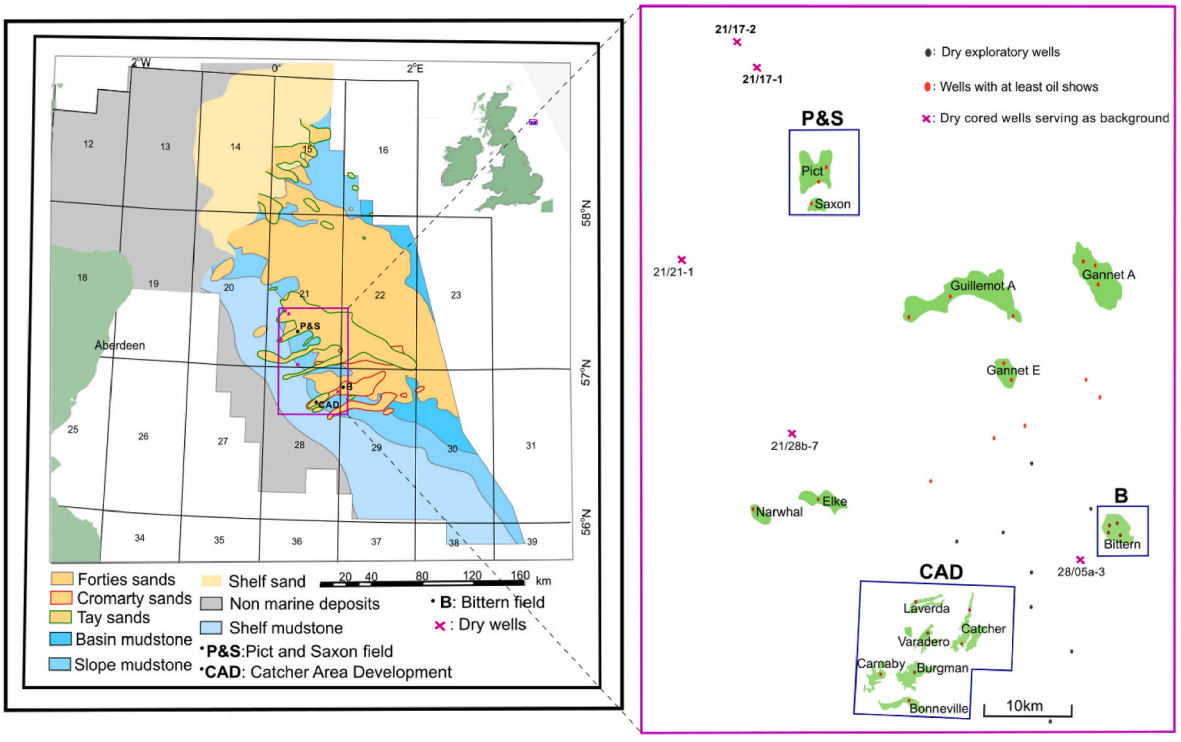

Fig. 1. Regional map highlighting the distribution of Tay, Cromarty and Forties sandstone members in the Central North Sea. The location of the Bittern field and the Catcher Area Development (CAD) is also highlighted. Well location for all the cores obtained from the oil fields and dry wells (background samples) are shown.

Table 1
Reservoir and fluid properties for the Bittern and Catcher Area Development (CAD) fields under study together with details of well cores sampled for magnetic analysis. These data were compiled using details obtained from well reports and the core analysis. N/G is net to gross (sandstone to sediments) and N.A. stands for not available.

FIELDS/DRY WELL	Oilfield Top TVDSS, m (ft)	Gross Pay m (ft)	N/G (%)	Sandstone Member	Well Name	Core Length m (ft)	N/G (%) - Core	Reservoir Temp. (°C)	Stock Tank Density (°API)	pH
BITTERN	2020 (6628)	80 (246)	>90	Forties	29/01a-7	80(261)	~90	90	39	N.A.
				Forties	29/1b-5	35(115)	~90			N.A.
				Forties	29/1b-6	80(261)	~100			N.A.
CATCHER	1355 (4446)	125 (38.1)	~30	Cromarty Tay	29/09-1 28/09-1z	37(122) 18(60)	~20 ~70	59	31	7
BONNEVILLE	1066 (3498)	20.1 (66)	~40	Tay	28/09a-6	26(84)	~50	46	24	7
CARNABY	1024 (3358)	26.2 (86)	~60	Tay	28/09a-5A	15(48)	~90	42	22	7
DW-1				Forties	28/05a-3	11(37)	100			N.A.
DW-2				Tay	21/21-1	8(25)	100			N.A.
DW-3				Tay	21/17-1	27(89)	~90			N.A.
DW-4				Tay	21/28b-7	6(19)	100			N.A.

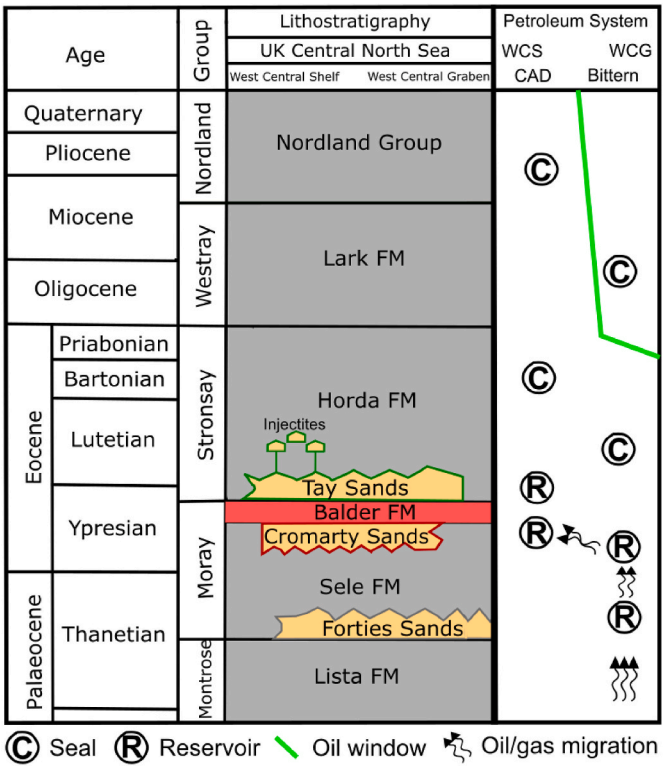

Fig. 2. Stratigraphic column highlighting the reservoir sandstones of interest, seals and timing of hydrocarbon generation and migration. Source rock (not shown) is the underlying Kimmeridge clay formation of the region (modified from Badejo et al., 2021c).

volumes of course grained material eastwards into the North Sea (Ahmadi et al., 2003). These deltaic and turbiditic sediments comprise the main Lower Tertiary sandstone reservoirs in the Northern North Sea Basin. Sourced from the underlying Upper Jurassic source rocks they contain approximately 25% of UK North Sea petroleum reserves (Kubala et al., 2003).

The Tay, Cromarty and Forties sandstones form part of the Horda, upper Sele and the lower Sele formations of the Central North Sea respectively (Fig. 2) (Ahmadi et al., 2003). The Sele formation deposition began ~56 Ma ago and is underlain by the blocky bioturbated mudstone of the Lista formation and overlain by the tuffaceous mudstone of the Balder formation. The Sele formation consists mainly of mudstones that are typically medium to dark grey, carbonaceous, commonly laminated and fissile. The Forties sandstone is its earliest major sandstone unit and occurred due to the uplift of the Scotland-Shetland landmass leading to the influx of sediments from the region (Ahmadi et al., 2003). This sandstone unit formed a North-westerly to South-easterly trending lobe with smaller west-south-west (WSW) – east-north-east (ENE) slope channels and deep basin deposits (Mudge, 2015; Robertson et al., 2013). The sandstone is fine to coarse grained, moderately sorted with homogenous structures (Ahmadi et al., 2003). Mudstone interbeds are common, however, the top and base of the Forties can be recognised by a rapid transition into thick Sele mudstones. In the study area, the Forties sandstones are mainly inputs from the western margins i. e the Forties platform that fed sediments into the region via W-E to WSW-ENE trending channels (Eldrett et al., 2015). These exists mainly as basin floor fans with minimal slope channels that thins rapidly to the west of the Bittern field towards the CAD region where it exists only in its eastern margins. It should be noted however that the main South-easterly trending Forties fan system may have also contributed to the sand layer of the Bittern area (Mudge, 2015). The gross thickness of Forties sands is ~100 m in the Bittern area and it thins to less than 10 m in the Catcher field. Overlying the Forties sand, is the less extensive Cromarty sandstone of the upper Sele formation (Robertson et al., 2013). This sandstone unit was sourced from the Westerly Forties platform and deposited in the region as isolated near W-E slope channels extending into the deeper basin (Mudge, 2015; Robertson et al., 2013). It may also contain some slump/debris flow deposits (Mudge, 2015). Compared to the Forties channels, the Cromarty sandstone extended further west in the region and is present in all the wells drilled in the CAD region. It is generally made up of fine grained clean poorly consolidated sands that are interbedded with grey carbonaceous mudstone (Ahmadi et al., 2003).

Overlying the Sele formation is the transgressive Balder formation (deposition was from ~55 Ma to ~ 53 Ma ago) comprising multi-coloured laminated shales, tuffs and coals (Ahmadi et al., 2003). This layer forms a good seismic marker horizon due to the presence of tuff that Results in significant acoustic impedance with the surrounding formations, making its mapping in the region easy and highly accurate

(Ahmadi et al., 2003). The overlying Horda formation deposition began ~53 Ma and comprises a thick sequence of green to grey hemipelagic mudstones together with the coarse grained poorly consolidated Tay sandstone (Jones et al., 2003). In the study area, the Tay sandstone was deposited on a Horda formation that was unconformable due to Tertiary faulting event and salt induced highs and lows (Jones et al., 2003; Stewart, 1996). This together with the diminished sediment supply to the region resulted in slope deposits that accumulated mainly in areas of tectonically induced lows e. g the hanging walls of the Tertiary faults (Robertson et al., 2013). The Tay sands are mainly found in the CAD region and does not extend into the deeper Bittern area. The Tay and the underlying Cromarty sandstone formed an injectite complex due to a seismically induced large scale dewatering event that occurred in the mid-late Eocene period (Gibson et al., 2020). This injectite complex consist of fully to partly injected and remobilized sands that forms a significant part of the petroleum system of the CAD region.

3. Sampling and experimental methodology

3.1. Sample collection

81 samples were collected from the Bittern sandstones, with an additional 60 samples from the CAD sandstones – all cores are archived at the British Geological Survey Core Store, Keyworth, UK. These cores are from three Bittern wells through the Cromarty and Forties sandstones, and four CAD wells, two from the Catcher field (through the Cromarty and Tay sandstones) and the two others from the Carnaby and the Bonneville field both through the Tay sandstones (Table 1). These sandstone sections and those from an additional four dry wells (26 samples in total) were generally sampled every 1–2 m depending on their length and observed homogeneity. The dry wells' cores were from similar stratigraphic level to the oilfield cores but were classified as dry due to: i) absence of hydrocarbon stains throughout the well section, ii) the information provided in the core reports after analysing for oil stains, and iii) the wells locations were at least 3 km away from any known hydrocarbon accumulation/show; three were >6 km distant.

3.2. Rock magnetic experiments

Rock magnetic experiments were carried out on all 167 core samples to determine their magnetic susceptibility and minerology. No one magnetic measurement can fully characterise a sample, therefore, it is necessary to apply a suite of different magnetic experiments, e.g., magnetic susceptibility, hysteresis and thermomagnetometry.

We measured bulk magnetic susceptibility, χ (magnetic field applied = 200 A/m), and hysteresis loops (applied field intensity = 500 mT) for the 167 samples using the Agico MKF1-Kappabridge and the Princeton Measurements Vibrating Sample Magnetometer (VSM) respectively at Imperial College London, UK. Magnetic susceptibility, χ is a quick measurement technique to determine the tendency of a material to be magnetized in the presence of magnetic field. Hysteresis loops help discriminate between ferromagnetic minerals (*sensu lato*), e.g., magnetite and pyrrhotite and paramagnetic minerals e.g., pyrite and siderite. The ferromagnetic contribution is quantified via the saturation remanent magnetization, M_{rs}, while the paramagnetic contribution can be quantified using the high-field susceptibility, χ_{hf} (Fig. 3).

To help identify the magnetic minerology, non-destructive low-temperature magnetometry (LTM) and high-temperature susceptibility (HT-χ) experiments were carried out on 40 (19 and 21 from Bittern and CAD respectively) and 109 (71 and 38 from Bittern and CAD respectively) of the oilfield samples respectively. LTM and HT-χ were also measured for 10 and 21 of the background samples respectively. LTM enables the identification of low-temperature phase transitions which are mostly unique to a magnetic mineral, e.g., the Verwey transition of magnetite at ~120 K (Verwey, 1939). LTM was performed using Quantum Design Magnetic Properties Measurement System (MPMS)

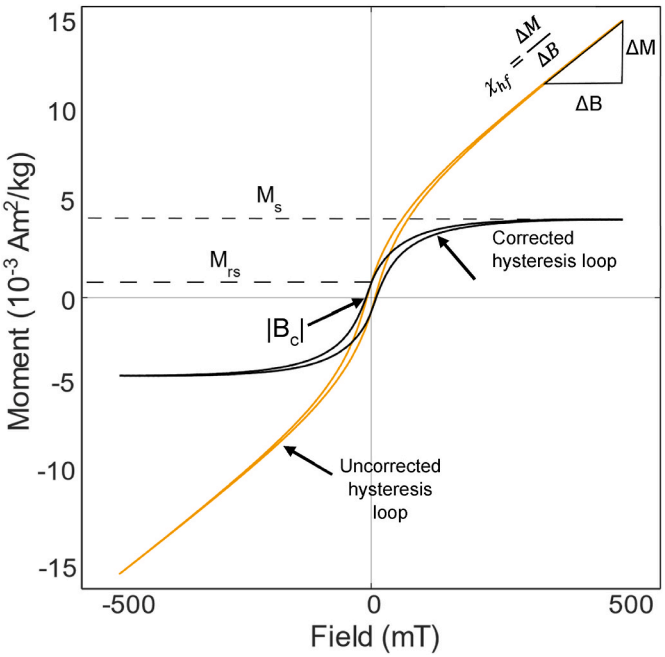

Fig. 3. An example hysteresis loop, sample DW-21-989 from the analyses. Here we highlight the saturation magnetization M_s, remanence magnetization M_{rs} coercive force B_c, and high field susceptibility χ_{hf}. Corrected hysteresis loop describes the ferromagnetic response of the sample in the presence of a field, while the uncorrected hysteresis loop describes the combined ferromagnetic, paramagnetic and diamagnetic response of a sample in the presence of a field.

instruments located at The Institute for Rock Magnetism, University of Minnesota, USA, Imperial College London, and Australian National University 'ANU' Canberra, Australia. A series of measurements were carried out: 1) Field-Cooled (FC) warming – cool the sample to 20 K in a field of 2.5 T, followed by warming to 300 K in zero field whilst measuring the remanence, 2) Zero-field Cooled (ZFC) warming, similar to the FC protocol, except that the field of 2.5 T is applied at 20 K after cooling in zero field, and 3) the Room-Temperature Saturation Isothermal Remanence Magnetization (RT SIRM) cycling measurement which involves inducing a remanent magnetization at 300 K in a field of 2.5 T, followed by measuring the remanent magnetization as it is first cooled to 20 K (RT $SIRM_{cooling}$) and then warmed to 300 K (RT $SIRM_{warming}$), both in a zero field environment.

HT-χ measurements were conducted at Imperial College London, and the Institute for Rock Magnetism using an Agico MFK1 Kappabridge with heating between room temperature and 700 °C in argon. HT-χ measurements helps to identify magnetic minerals through their phase transitions or their alteration characteristics, e.g., siderite rapidly alters on heating above 300 °C to magnetite resulting in a significant increase in magnetic susceptibility (Pan et al., 2000).

3.3. Mössbauer spectroscopy

Mössbauer spectra were measured for a limited number of samples: three from Bittern, three from CAD and two dry well samples. The samples were selected based on their paramagnetic responses, and it was ensured that a sample in the upper limit of χ_{hf} values in each region was included. Samples with low χ_{hf} were also selected. Room and low (between 18 K and 5 K) temperature Mössbauer spectra were measured for these samples using the Co. MS6 Mössbauer spectrometer, with Janis SVT-400 Nitrogen-shielded liquid Helium cryostat at the Institute for Rock Magnetism. Mössbauer spectroscopy was used as a complementary quasi-magnetic mineral identification technique due to its ability to distinguish amongst magnetic minerals (Dyar et al., 2006).

3.4. XRD analysis

X-Ray diffraction (XRD) analysis was used to help identify and quantify the different minerals present in fifteen and four semi-randomly selected oilfield and background samples respectively. Samples with both high paramagnetic and low paramagnetic responses were measured at the Natural History Museum (NHM). About 1 g of sample was grounded to a grain size of <30 μm. The measurement was carried out using the PanAnalytical XRD ML Scan device at 2Θ (theta) angles between 3.5° and 120° using X-ray radiation from a copper anode at 40 kV and 40 mA. Mineral identification and quantification via Rietveld analysis (Doebelin and Kleeberg, 2015) were carried out on the acquired X-ray diffraction pattern using the Highscore Plus from Malvern Software and the BGMN-Profex respectively, and the PDF-2 database from International Centre for Diffraction Data (ICDD). Crystal structure data for mineral quantification were taken from the Inorganic Crystal Structure Database (ICSD) and Profex-BGMN together with additional data for disordered smectite from Ufer et al. (2004).

3.5. $\delta^{13}C$ isotope analysis

Stable isotope analysis was carried out on 10 sandstones samples, five from the CAD area and five from the Bittern fields at Iso-Analytical Ltd., Cheshire, UK. This analysis was carried out in order to determine the source (thermogenic or biogenic) of the carbon in siderite found in these sandstones. The samples had been identified to contain >0.5% siderite. Magnetic separation was carried out on these samples using the Frantz magnetic separator to increase the concentration of siderite. The magnetic extracts were weighed into ExetainerTM tubes and then flushed with 99.995% helium. After flushing, phosphoric acid was added to the samples at 90 °C for no less than 48 h to produce Carbon dioxide from the carbonate. Carbon dioxide produced from samples was then analysed by Continuous Flow-Isotope Ratio Mass Spectrometry (CF-IRMS). Carbon dioxide was sampled from the ExetainerTM tubes into a continuously flowing He stream using a double holed needle. The CO_2 was resolved on a packed column gas chromatograph and the resultant chromatographic peak carried forward into the ion source of a Europa Scientific 20-20 IRMS where it was ionized and accelerated. Gas species of different masses were then separated in a magnetic field and simultaneously measured using a Faraday cup collector array.

4. Results

4.1. Room-temperature magnetic susceptibility and hysteresis measurements

A summary of the mass-normalized room temperature susceptibility and hysteresis data are shown in Table 2. The magnetic susceptibility values are highly variable in the oilfield samples ranging between 1.4×10^{-9} m^3/kg and 163×10^{-9} m^3/kg (Fig. 4a). The background samples also display variability in magnetic susceptibility with values ranging from 1.7×10^{-9} m^3/kg to 67.5×10^{-9} m^3/kg. The significantly lower range and maxima observed for the dry well samples as compared to the oilfield samples suggests sedimentary diagenesis after oil emplacement. The observed susceptibility values are similar to those from the literature, e.g., Bridport sandstone, Wessex Basin (Abubakar et al., 2020) and Lunde formation of the Northern North Sea (Hounslow et al., 1995).

The oilfield samples are generally ferromagnetically weak with highly variable saturation remanence, M_{rs} values. The background samples are also magnetically weak but have significantly higher M_{rs} values compared to the oilfield samples (Table 2). The oilfield samples' coercivity values, B_c are also slightly lower than that of the background samples, although all the samples are dominated by low coercivity magnetic minerals. The M_{rs} and B_c values are similar to the values measured by Emmerton et al. (2013) for oil stained sandstone samples from sedimentary basins in Columbia, Canada, Indonesia and the UK, and Badejo et al. (2021a) for oil-stained and unstained sandstone samples from the West Central Graben, North Sea, UK.

The background samples present a good correlation between the magnetic susceptibility, χ and the M_{rs} values (R-squared of 0.89) (Fig. 4a) unlike the oilfield samples (R-squared of 0.20). This shows the general dominance of the ferromagnetic response in the background samples unlike the oilfield samples. Also, the high field susceptibility χ_{hf} and the χ values average to a significantly higher value in the oilfield samples as compared to the background samples (Table 2). The paramagnetic response dominates a significant number (over 30%) of oilfield samples (Fig. 4a) and appears to be randomly distributed along the reservoir section (Fig. 4b).

Table 2
A summary of the hysteresis parameters and magnetic susceptibility χ values obtained for the oilfield and background samples. Magnetic minerals identified are also included. Mag, FeS, TiO and Hem stands for magnetite, iron sulphides, titanium-rich iron-oxides and hematite respectively. *n* is the number of samples.

FIELD/DRY WELL	Well name	*n*	Mean χ 10^{-9} m^3/kg	Range χ 10^{-9} m^3/kg	mean M_{rs} $10^{-3}Am^2/kg$	Range M_{rs} $10^{-3}Am^2/kg$	Mean B_c mT	Mean χ_{hf} 10^{-9} m^3/kg	Range χ_{hf} 10^{-9} m^3/kg	Major magnetic mineral
BITTERN	29/01a-7	40	26	160	0.06	0.17	9	29	210	**Siderite**[a], FeS, Mag, TiO
	29/1b-5	16	23	51	0.07	0.08	8	22	58	**Siderite**[a], FeS, Mag, TiO
	29/1b-6	25	16	37	0.07	0.11	8	16	38	**Siderite**[a], FeS, Mag, TiO
CATCHER	29/09-1	8	11	11	0.14	0.13	9	3.6	11	Mag, TiO
	28/09-1z	13	4.9	9	0.10	0.20	9	0	8	Mag, TiO
BONNEVILLE	28/09a-6	23	41	105	0.17	0.50	8	51	300	**Siderite**[a], FeS, Mag., TiO
CARNABY	28/09a-5A	16	23	96	0.10	0.13	9	19	119	**Siderite**[a], FeS, Mag., TiO
DW-1	28/05a-3	6	4	10	0.04	0.07	10	3	12	Mag, TiO, Hem
DW-2	21/21-1	8	2	51	0.40	0.69	11	11	35	Mag, TiO
DW-3	21/17-1	9	27	59	0.48	0.92	14	11	15	Mag, TiO
DW-4	21/28b-7	3	13	15	0.17	0.08	13	9	18	Mag, TiO

[a] Siderite is present in significantly higher concentrations than the other magnetite minerals; up to two orders of magnitude higher.

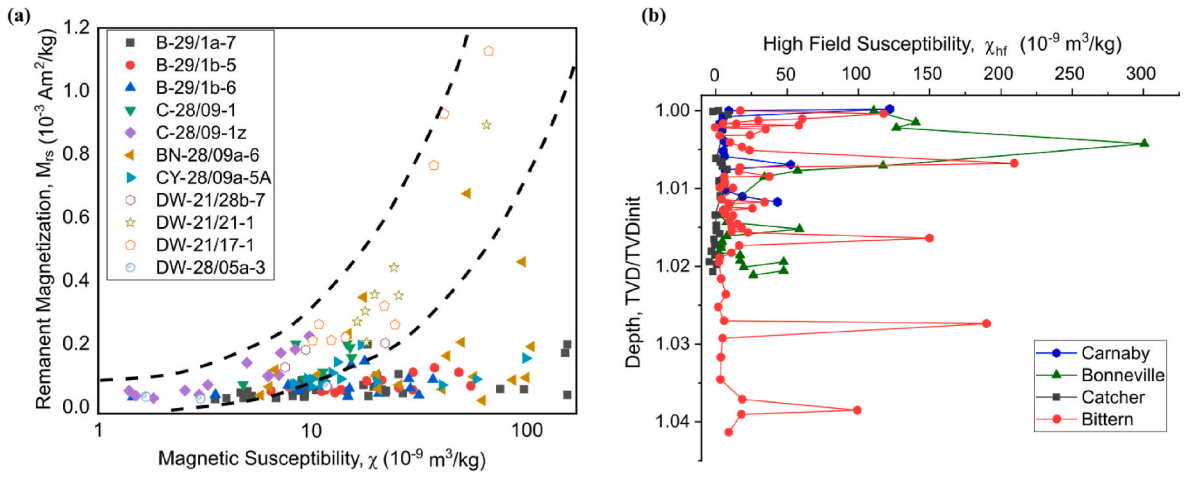

Fig. 4. a) The relationship between the magnetic remanence and the magnetic susceptibility for the background (hollow symbol) and the oilfield (solid symbols) samples. The background samples present a good correlation between these two parameters (R-squared value of 0.89) while the oilfield samples present a weak correlation (R-squared value of less than 0.20). The region within the dashed lines is the approximate region of ferromagnetic dominance. As sample points move away from this region to the right, the paramagnetic proportion increases and begins to dominate the magnetic signature. b) Variation in high field susceptibility as a function of sample location. Note regions of enhanced χ_{hf} values in some of the oilfields. TVD and TVDinit stands for true vertical depth and shallowest sample's true vertical depth respectively.

4.2. Low temperature magnetometry

Low-temperature warming and cooling curves were obtained for samples from the Bittern, Catcher, Bonneville, Carnaby oilfields and background samples (Figs. 5 and 6). For the FC and ZFC warming curves, a sharp drop in remanence was generally observed on warming between 10 K and 37 K for the highly paramagnetic oilfield samples with a ratio of $SIRM_{FC@10K}$ to $SIRM_{ZFC@10K}$ of greater than three and up to eight, e.g., Bit-2100 (Fig. 5b) and Bon-1180 (Fig. 5h). Also, the $SIRM_{FC@10K}$ generally increased with increasing paramagnetic response (Figs. 5 and 6). This signature is indicative of siderite's Néel transition temperature (Jacobs, 1963). All the oilfield samples with significant paramagnetic proportion as identified via χ_{hf} displayed this low-temperature behaviour indicative of siderite. This signature also appears to diminish with a drop in paramagnetic response and disappears for samples that are dominantly diamagnetic. Note that none of the background samples (Fig. 6h and k); irrespective of their paramagnetic responses, showed any signs of the presence of significant amounts of siderite.

The RT-SIRM curves for both the oilfield and background samples generally presented a discontinuity or change in slope between 110 K and 130 K. This is indicative of magnetite (for transition at about 120 K) (Verwey, 1939), or maghemite/titanomagnetite (as transition shifts away from 120 K (Moskowitz et al., 1998; Muxworthy and McClelland, 2000). e.g., Cat-1564 (Fig. 6e) and DW-17-1532 (Fig. 6h).

The RT SIRM cooling curves for several oilfield samples, and background samples presented a subtle discontinuity in remanence at about 263 K, e.g., DW-17-1532 (Fig. 5h). This is indicative of hematite (Morin, 1950). Emmerton et al. (2013) also observed the presence of hematite in sandstone samples from the Wessex Basin, UK, Athabasca, Saskatchewan, Canada, and Kabungkan and Lawele, Buton Island, Indonesia. There was a significant increase in RT-SIRM on cooling between 300 K and 20 K for the majority of the samples, > 40% and up to 100%, e.g., Bit-2100 (Fig. 5b). This is likely due to the presence of low to intermediate composition titanohematite (Sprain et al., 2016).

4.3. High-temperature susceptibility (HT-χ) measurements

HT-χ curves for the highly paramagnetic oilfield samples presented a rapid and continuous increase in magnetic susceptibility above 300 °C with Curie temperatures of between 560 °C and 580 °C. e.g., sample Bit-2112 (Fig. 5f) and Car-1085 (Fig. 5l). An increase in susceptibility of up to three orders of magnitude was observed for the most paramagnetic samples. These samples generally presented Hopkinson peaks just below the Curie temperature of magnetite. This is the thermomagnetic behaviour of siderite at these conditions (Pan et al., 2000). Siderite oxidizes to magnetite and/or other iron-oxides at temperatures above 300 °C. Similar observations were made by Badejo et al. (2021a) for oil stained highly paramagnetic samples from the West Central Graben in the North Sea.

The HT-χ curves for some dominantly diamagnetic samples presented a rapid drop in susceptibility above 500 °C with Curie temperatures of between 558 °C and 562 °C. e.g., Cat-1429. (Fig. 6c). These samples did not present any substantial increase in susceptibility that can be attributed to mineral alteration (Fig. 6f). This suggests the presence of magnetite, native to these samples.

The HT-χ curves for some oilfield samples, mostly proximal or at the oil-water contact (OWC), presented a rapid increase in susceptibility at about 200 °C with a Curie temperature of ~270 °C, This is an indicator for the presence of hexagonal pyrrhotite (Rochette et al., 1990). Also, some of the Bittern field samples close to the oil-water contact presented a rapid and near instantaneous increase in susceptibility at temperatures anywhere between 250 °C and 280 °C, this signature was irreversible as observed from cycling experiments. We suggest that this mineral may be a paramagnetic iron sulphide and the rapid increase in susceptibility observed may be due to its conversion to a ferromagnetic (*sensu lato*) mineral. Iron sulphides are generally observed in significantly higher concentration around the OWC due to higher biodegradation rates observed in these locations (Badejo et al., 2021b, 2021c).

4.4. Mössbauer results

Mössbauer spectra were obtained for eight samples at 295 K and seven samples at temperatures between 5 K and 18 K. Each room temperature spectrum was successfully fitted with two quadrupole doublets, i.e., paramagnetic signals. For the low temperature spectra, only the oilfield samples that were highly paramagnetic at room temperature displayed sextets, i. e, ferromagnetic (*s.l.*) behaviour, in addition to the two quadrupole doublets observed in all the samples. (Fig. 7). These three highly paramagnetic oilfield samples had isomer shifts 'IS', quadrupole splitting 'QS' and hyperfine splitting 'B_{hf}' of between 1.34 mm/s and 1.37 mm/s, 2.02 mm/s and 2.06 mm/s and 17.7 and 18.0 T respectively (Table 3) which are indicative of siderite (Stevens et al.,

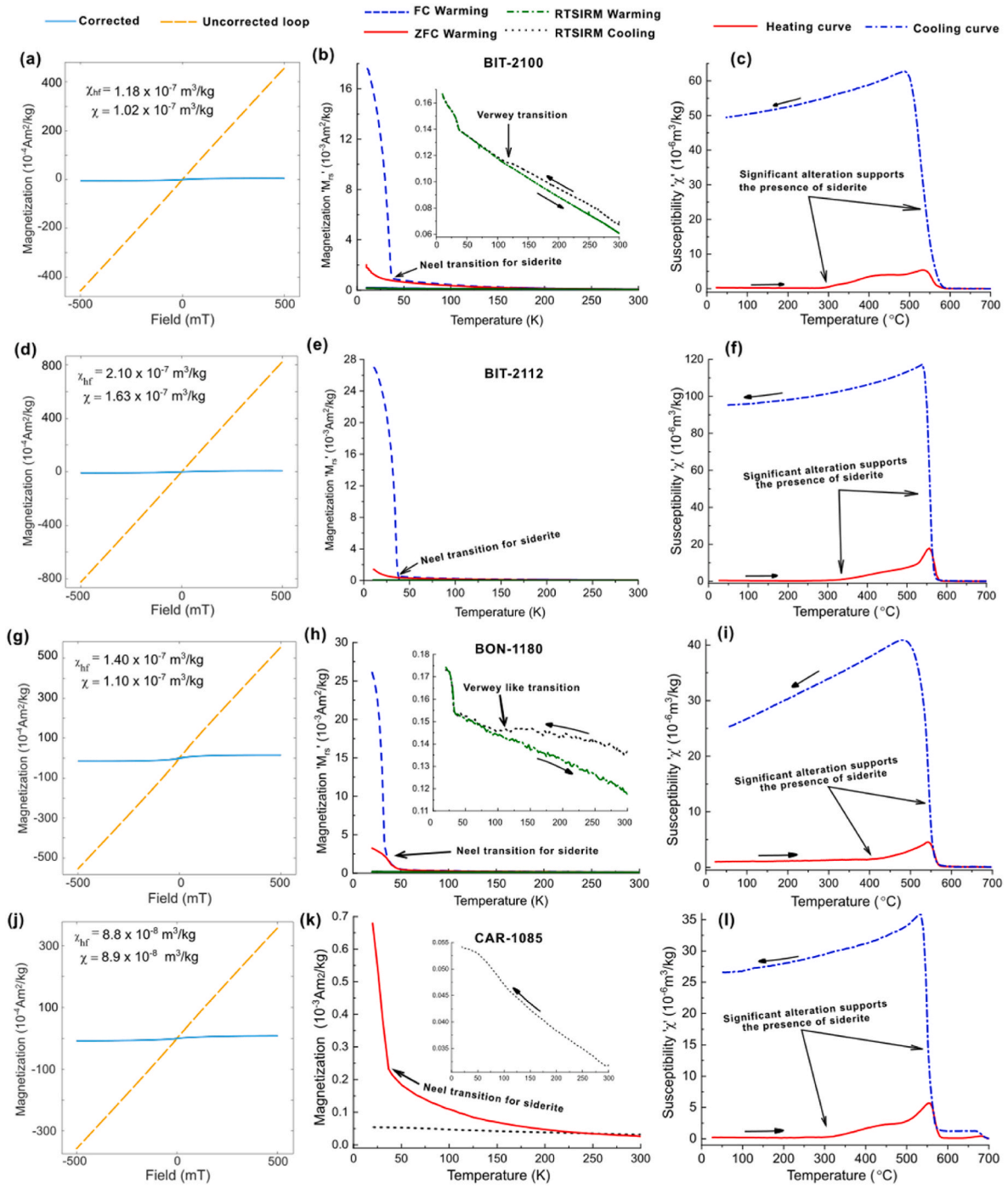

Fig. 5. Example of hysteresis, LTM and HT-χ measurement Results for oilfield samples with significant quantities of siderite present; Bit-2100, Bit-2112, Bon-1180 and Car-1085 are shown on figure (a, b & c), (d, e & f), (g, h & i) and (j, k & l) respectively. These measurement curves suggest the presence of siderite, iron sulphides, magnetite, Ti-rich iron oxides and hematite as highlighted.

1998). Also, the 'IS' and 'QS' values (Table 3) for one of the doublets of the room temperature Mössbauer spectra of these three samples is indicative of the presence of siderite (Dyar et al., 2006; Stevens et al., 1998). Conversely, the IS and QS values for the two quadrupole doublets observed for the Mössbauer spectra of the oilfield samples with low paramagnetic proportions and the background samples indicated only silicates and/or pyrite (Dyar et al., 2006; Stevens et al., 1998).

4.5. XRD analysis

XRD analysis found that the minerology of all the samples is very similar with the identification of quartz, k-feldspar, plagioclase, illite, kaolinite, siderite, calcite, pyrite and halite phases (Table 4). Siderite appears to be the main distinguishing mineral between the oilfield and the background samples. In the oilfield samples, the quantity of siderite as determined from the spectra is generally proportional to the χ_{hf}, with the concentration between 0.5 and 11% (Fig. 8).

However, for the diamagnetic oilfield and the background samples, siderite was generally absent or only just identified but not quantifiable (<0.3%). All the other minerals are present in both sample groups in significant amounts. Where present, kaolinite appears to be associated with high siderite content. Huggett (1996) reported similar

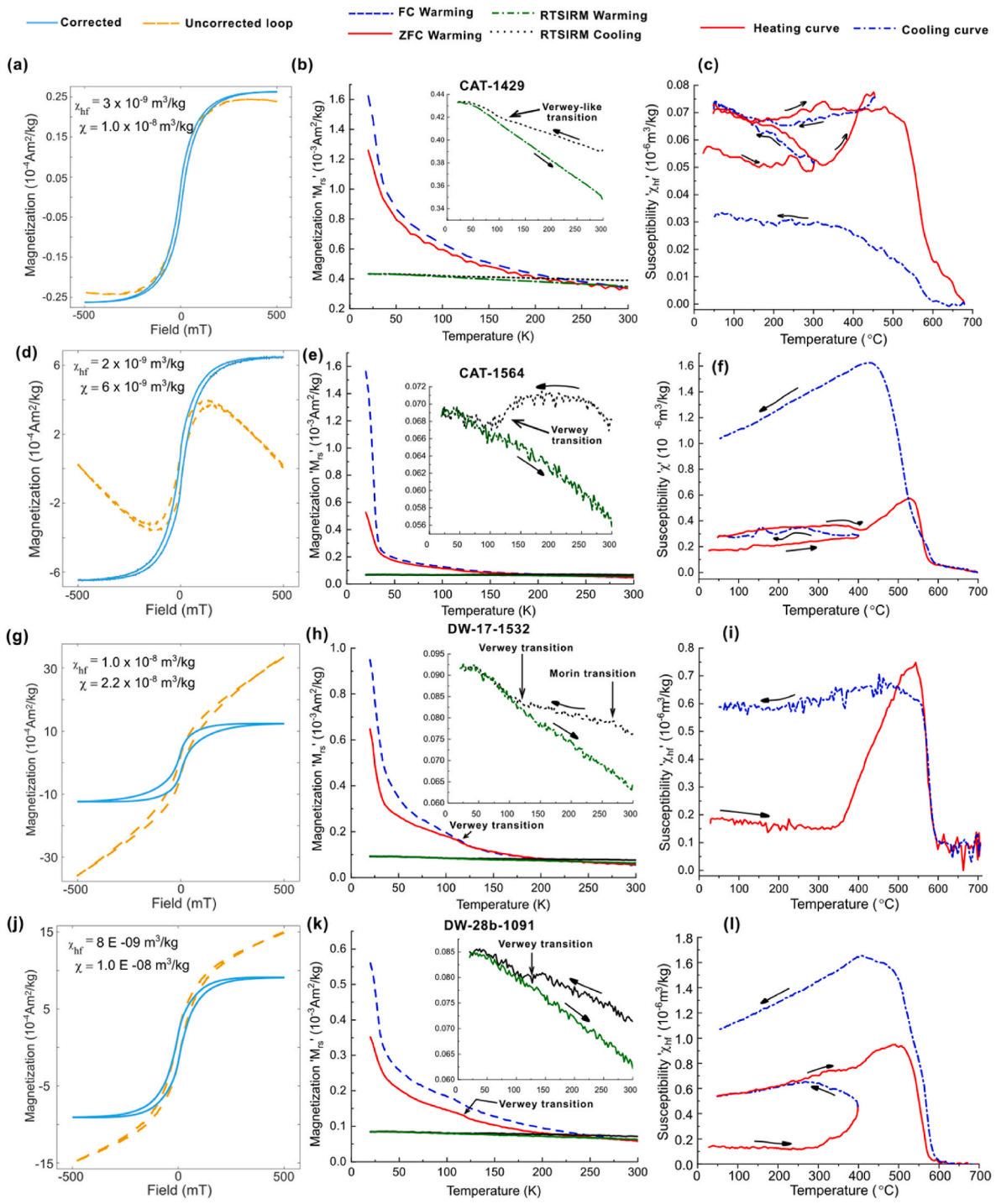

Fig. 6. Representative examples of hysteresis, LTM and HT-χ measurement Results from the siderite poor regions; Catcher oilfield and the background sandstones. Cat-1429 and Cat-1564 results for the oilfield are shown on figure (a, b & c) and (d, e & f) respectively, while DW-17-1532 and DW-28-1091 for the background sandstones are shown on figure (g, h & i) and (j, k & l) respectively. Note the absence of a siderite's Néel transition on the FC-ZFC curves and the insignificant increase in magnetic susceptibility due to mineral alteration as compared to the siderite rich sample.

mineralogical distribution for Tertiary sandstones from the UK Central North Sea region.

4.6. $\delta^{13}C$ isotope analysis

Results from stable isotope analysis indicates that the siderite has a wide range of $\delta^{13}C$ values; from – 15.7 to 14.1‰ (VPDB or Vienna Pee Dee Belemnite standard) (Fig. 9). For the Carnaby field, the siderite samples' $\delta^{13}C$ ranges between −15.7 and −8.0‰ suggesting its formation from HCO_3^- (or CO_2) made up of isotopically lighter carbon (relative to the standard). The Bonneville samples, however, contains siderite form from HCO_3^- (or CO_2) of different sources, with $\delta^{13}C$ ranging between −9.0 and 11.8‰. Two-thirds of the samples are made up of isotopically light carbon ($\delta^{13}C$ values of between −9.0 and −10.0‰), and the rest is formed from HCO_3^- (or CO_2) enriched in ^{13}C ($\delta^{13}C$ value of 11.8‰). The Bittern samples consist of siderite with $\delta^{13}C$ ranging between 6.8 and 14.1‰, suggesting their formation from HCO_3^- (or CO_2) enriched in ^{13}C. The $\delta^{18}O$ values for the samples range

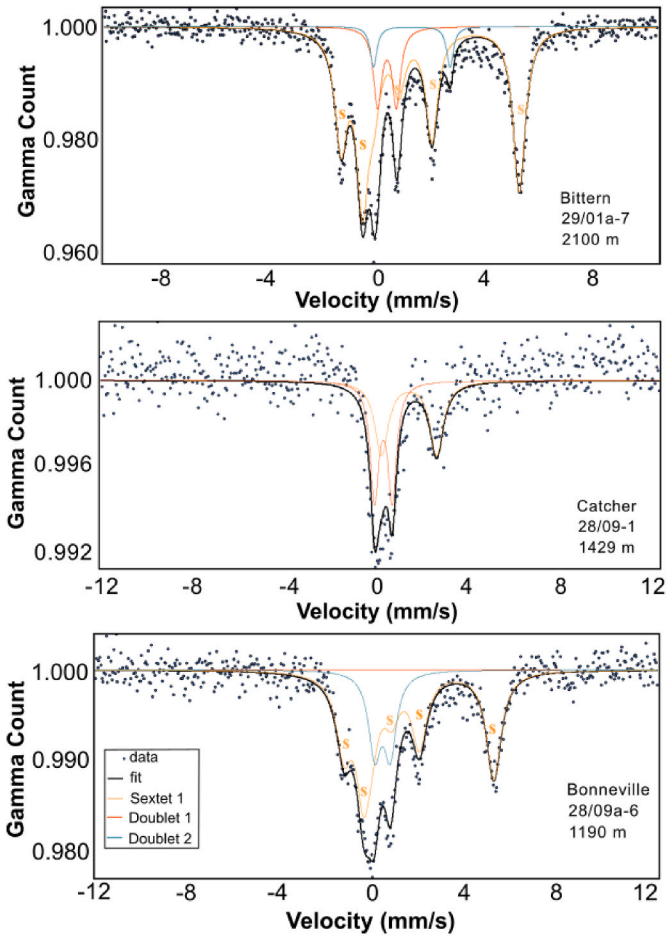

Fig. 7. Low temperature Mössbauer spectroscopy Results for oilfield samples; Bit-2100, Cat-1429 and Bon-1190 reveals the presence of siderite (labelled as 's') in the two samples with high paramagnetic response and its absence from the sample with low paramagnetic response. Depths are shown in TVDSS.

Table 3
Mössbauer parameters for the magnetic hyperfine split sextet (low temperature spectra) and a quadrupole doublet (room temperature spectra) obtained for samples from Bittern and Bonneville. These parameters fit to siderite. IS stands for isomer shift and QS stands for quadrupole shift. Note that all isomer shift data are given with reference to metallic iron.

SAMPLE NAME	Low Temperature (5–18 K)			295 K	
	'IS' (mm/s)	'QS' (mm/s)	Hyperfine field (T)	'IS' (mm/s)	'QS' (mm/s)
Bit-2100	1.34	2.02	18.0	1.22	1.83
Bon-1190	1.37	2.06	17.7	1.21	1.83
Pure siderite	1.38	2.02	18.5	1.22	1.80

between −6.0 and −1.8‰ (VPDB); −6.0 to −5.4‰ for Bittern; −4.0 to −2.4‰ for Bonneville; and −2.2 to −1.8‰ for Carnaby.

5. Discussion

Rock magnetic experiments identified a variation in the magnetic signature of the oilfield sandstones and the nearby background sandstones. Unlike the oilfield sandstone, the background sandstones magnetic response is dominated by its ferromagnetic components. There is a significant reduction and increase in the ferromagnetic and paramagnetic signature respectively in the oilfield sandstones as compare d to the background sands. However, the increased paramagnetic response is not uniform. The oilfield sandstones have a wide range of paramagnetic/diamagnetic response with a significant number of them having very low paramagnetic responses, hence low concentration of paramagnetic minerals. Mineralogically, the background sandstones contained magnetite, hematite and Ti-rich iron-oxides while the oilfield's magnetic environment is more diverse with magnetite, hematite, Ti-rich iron oxides, iron sulphides and siderite identified. The signature of magnetite and hematite has been significantly diminished in the oilfield sands. Here, siderite is present in a significantly higher concentration than the other magnetic minerals; up to 10%. All the other magnetic minerals are present in trace amounts. From the RT-SIRM data obtained, we estimate a maximum possible concentration for individual ferromagnetic minerals of 500 ppm. For the paramagnetic iron sulphides (Table 4 and Fig. 10), concentrations of up to 0.3% has been estimated. The magnetic Results together with the XRD analysis also suggests that χ_{hf} and χ, can be used to approximate the quantity of siderite in the samples (Fig. 8) and hence, provides a quick estimate for the siderite content in similar environments. Isotope analysis revealed that siderite found in the Bonneville and Carnaby fields is isotopically light with respect to its carbon content (with $\delta^{13}C$ values averaging to −6.2‰ (VPDB)) while that of Bittern is heavier (with $\delta^{13}C$ values averaging to −9.9‰ (VPDB))

5.1. Magnetic signature of the oil reservoir sands – what does it tell us?

Analysis of the magnetic Results suggest a hydrocarbon induced replacement of ferromagnetic components such as magnetite, hematite by room-temperature paramagnetic minerals such siderite, pyrite and hexagonal pyrrhotite. Such a response is predicted by thermodynamic modelling (Burton et al., 1993); however, the concentration of paramagnetic minerals formed suggests that other Fe^{2+} sources are required, not just ferromagnetic mineral replacement. These sources could be aqueous Fe^{2+} (Machel and Burton, 1991) and/or Fe-rich clay minerals (Bello et al., 2021; Macaulay et al., 1993; Wilkinson et al., 2000). Fe-rich clays are common in North Sea sandstones (Wilkinson et al., 2006) and have been identified in the samples of this study (Table 4).

Siderite is the dominant diagenetic product after oil emplacement in the Bittern, Bonneville and Carnaby fields (Table 4 and Fig. 10). However, for the Catcher field with similar reservoir and fluid properties, this is not the case. This shows that although the diagenetic conditions required for the formation of siderite is promoted by hydrocarbons, the factors affecting the thermodynamics and kinetics must be considered carefully to predict its presence and concentration in a petroleum reservoir. These factors i.e., total organic content (TOC), bicarbonate ion, sulphide ion, aqueous Fe^{2+} concentration, pH and Eh values (Burton et al., 1993; Larrasoaña et al., 2007) must be considered in terms of variability in these fields to better understand the processes in play.

5.2. Variation of siderite within the oil reservoir sands: observations and sources

In the Bittern field, siderite appears to be present in over 80% of the oil-leg sandstones in the eastern section of the field, although its concentration is highly variable (trace to >10%). It is also present in a lesser, but significant quantity in the water leg of this section. However, siderite appears to diminish to the west of this oilfield. This is reflected in the reduction in χ_{hf} and χ (Table 2) and the thermomagnetometry data. For the Catcher field, the data suggest a general absence of siderite in the reservoir sands. Siderite is however present in significant amounts in the Bonneville and Carnaby fields with up to 5% been identified.

To try and understand the factors which control the variability in siderite precipitation in the oilfields, we must first assume that the geochemical conditions in a petroleum reservoir pre-hydrocarbon infiltration is homogenous. This assumption appears reasonable when we consider the apparent similarity in mineralogy of the background sandstones (Table 4). Machel (1995) showed that hydrocarbon changes

Table 4
XRD estimates of the minerals present in sandstone samples from the hydrocarbon reservoirs and dry wells. All values are in percentages. Tr stands for trace and represents estimates of minerals at < 0.3%. The micas present are illite, muscovite, biotite and potentially illite-smectite.

	Bit-2100	Bit-2105	Bit-2112	Bit-2129	Bit-2154	Bit-2178	Cat-1420	Cat-1564	Car-1080	Bon-1181	Bon-1200	D21-989	D17-1519	D17-1607	D21-1-995
Quartz	65	75	69	79	76	71	82	83	76	73	85	84	82	78	72
Plagioclase	9	6	7	8	7	11	5	3	3	9	6	6	5	7	11
k-Feldspar	10	9	7	8	6	9	9	9	13	11	7	8	9	11	11
Micas	3	6	1	2	1	2	1	1	3	2	1	1	1	2	3
Kaolinite	6	3	5	3	4	3			2			1	2	2	
Calcite	tr				tr		1	1	tr			tr	tr	1	tr
Siderite	7	1	11	tr	6	4	tr	tr	3	5	tr				tr
Pyrite	tr	tr		tr					tr					tr	
Halite	tr	tr	tr		tr	tr	tr	tr			0.6	tr			1

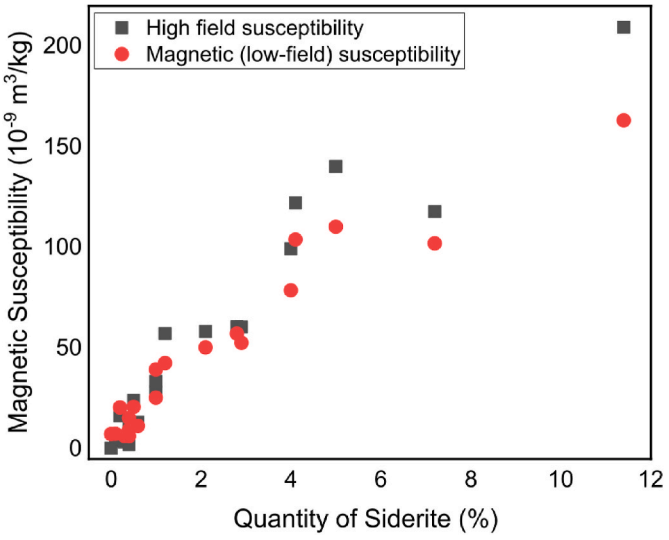

Fig. 8. The graph of susceptibility (χ and χ_{hf}) versus siderite concentration for oilfield samples reveals a good correlation (R-squared value of 0.92) between the two parameters.

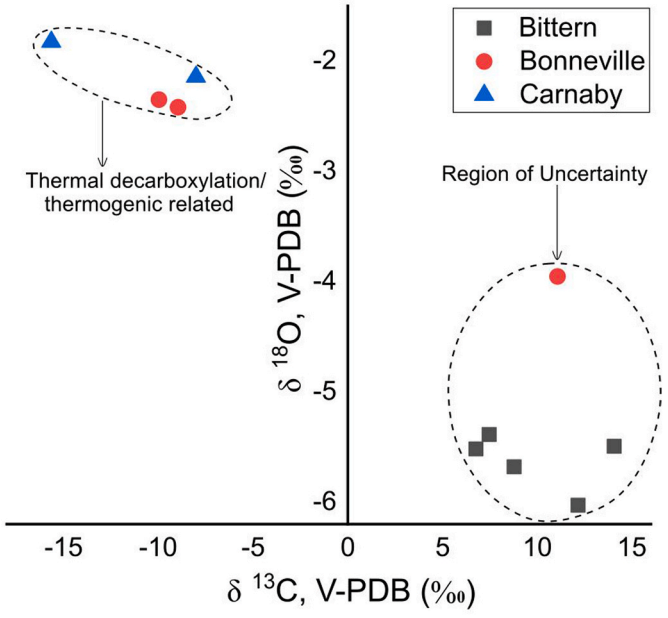

Fig. 9. Plot of $\delta^{18}O$ oxygen versus $\delta^{13}C$ carbon isotope composition for siderite under consideration. The plot reveals the likely sources of CO_2/HCO_3^- that reacted to form siderite in the Bittern, Bonneville and Carnaby oilfields.

the thermodynamic equilibrium and may result in the formation of minerals such as siderite, iron sulphides due to factors which include the introduction of H_2S and CO_2. For the oilfields in this area sulphur content is low (≪0.05% H_2S identified in the reservoir fluids) and it is likely that iron sulphide precipitation is restricted (Machel and Burton, 1991). In contrast, from the well reports, CO_2 is present in concentrations of up to 1.5 mol%. For migrating hydrocarbons, the availability of CO_2 for physical mixing and chemical reaction is likely affected by depth change. It is known that the solubility of CO_2 in formation water generally increases with depth (Zarghami et al., 2017; Zuo et al., 2013). Also, Smith and Ehrenberg (1989) have shown that the quantity of CO_2 existing in equilibrium with hydrocarbon fluids in clastic reservoirs is directly proportional to the depth of the reservoirs, and that the excess CO_2 leads to the precipitation of carbonates. Amongst the carbonates commonly found in sandstone reservoirs, siderite is the most likely to precipitates in a system if sufficient reacting cations are available (Campbell and Campbell, 2018). Therefore, for hydrocarbons migrating vertically, subject to the availability of Fe^{2+}, we would expect an increase in the concentration of siderite precipitated and potentially iron sulphides. As was mentioned earlier, in the oilfields of this study, Fe^{2+} is supplied by the in-situ pore water, existing ferromagnetic minerals and the dissolution of iron-rich clay minerals, e.g., mica etc (Bello et al., 2021; Wilkinson et al., 2000).

Other parameters such as Eh, pH and TOC, are unlikely to vary significantly within and between the oilfields in this study. TOC is likely be very similar due to the similarities in constituents of the hydrocarbons. Eh which is dependent on the presence of hydrocarbons and the hydrological and sedimentary conditions of the oilfields (Machel, 1995) is also likely to present very similar values. The present-day pH of the reservoir fluids as obtained from well reports (Table 1) are very similar, and suitable for siderite precipitation (Burton et al., 1993). Any significant variation in pH within these clastic reservoir systems is unlikely as its value is generally controlled by reactions between feldspars and clays dependent on depth (Smith and Ehrenberg, 1989). At temperatures less than about 110 °C, the introduction of hydrocarbons with its pH altering constituents such as CO_2, will engender this buffering process that generally involves the precipitation of carbonates (Hutcheon and Abercrombie, 1990; Smith and Ehrenberg, 1989).

To make the discussion around the precipitation of siderite less generic and more predictive, data from thermodynamic model developed by Burton et al. (1993); and Machel (1995) together with measured and modelled data of the controlling parameters are used to obtain a conceptual model (Fig. 11). The sediments under consideration are deep marine sediments (Ahmadi et al., 2003; Jones et al., 2003) where organic matter concentration during deposition is usually low (Roberts, 2015). Any organic matter present therefore likely degraded completely before the methanogenesis stage of near surface diagenesis explaining the general absence of siderite in the background sandstones (Table 2). Assuming steady state conditions, with continuous burial, siderite precipitation is unlikely to occur within the pH and E_h values (Fig. 11a(I)) (Burton et al., 1993; Hess, 1986; Railsback, 2006; Roberts, 2015), low

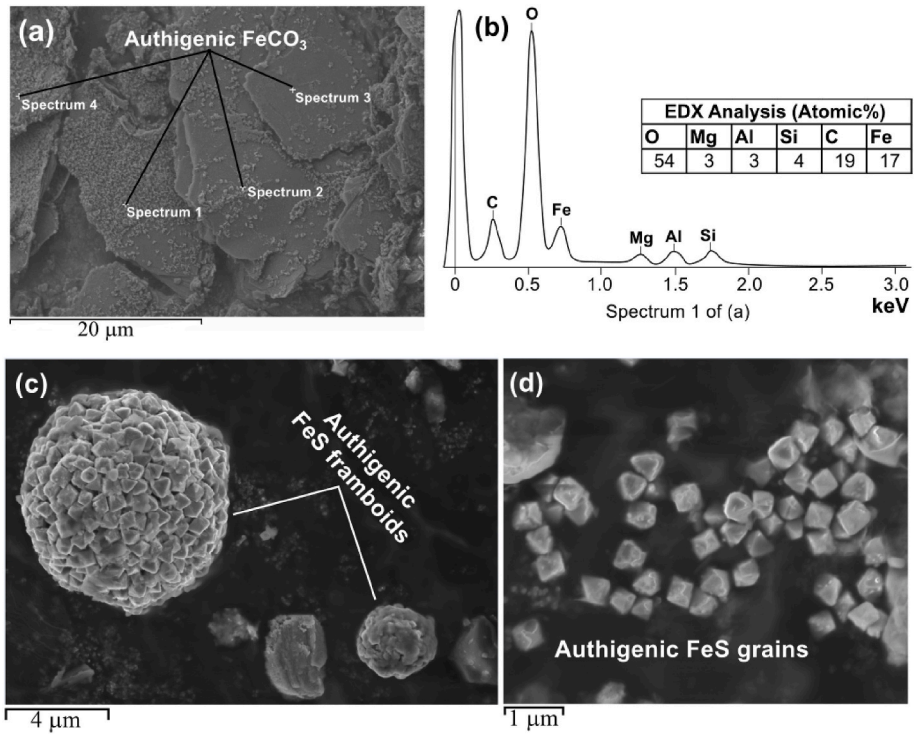

Fig. 10. Microscopic characterization of the a) platy like structure of siderite found in a Bonneville sample together with b) an example EDX spectrum from this location. All other spectra shown revealed similar composition. c) iron sulphide framboids and d) grains identified in sediments of CAD region.

TOC and the low concentration of HS^- and HCO_3^- normally encountered. HS^- and HCO_3^- concentrations are generally less than 1 ppm (or activities of HS^-, $aHS^- < 10^{-6}$) and 100 ppm (or $aHCO_3^- < 10^{-4}$) respectively in these sediments (Burton et al., 1993; Kuwabara et al., 1999; Miller et al., 2017; Oni et al., 2015). Note that E_h value is the least predictive amongst these parameters but is unlikely to go below – 0.5 V in the environment considered (Railsback, 2006). The introduction of hydrocarbons into the system (a(II) and (III)) increases the HS^-, HCO_3^- and the TOC whilst reducing the E_h values. According to the thermodynamic model developed by Burton et al. (1993); and Machel (1995), high sulphur content crudes (sulphur content of >0.5%) will generally have $aHS^- \gg 10^{-6}$, resulting in a drive towards the reaction of available Fe^{2+} in pore water, ferromagnetic minerals, and potentially other iron containing minerals to produce iron sulphides (Fig. 11a(II)) (Roberts, 2015). In this type of reservoirs, siderite precipitation is unlikely unless the concentration of the available Fe^{2+} exceeds the requirements of the available sulphides ions (Larrasoaña et al., 2007). However, for low sulphur crude (sulphur content ≪ 0.5%), e.g. The Bittern and the CAD fields of the UK Central North Sea, the precipitation of siderite is not hampered by iron sulphide precipitation and is the most likely magnetic mineral to form (Fig. 11a(III)) (Burton et al., 1993) if the CO_2 influx significantly increases the HCO_3^- concentration. Fig. 11b clearly depicts how the impact of CO_2 varies in lateral versus vertical migration with significantly more CO_2 becoming available for reaction as hydrocarbon migrates vertically due to reduction of its equilibrium partial pressure with depth (Smith and Ehrenberg, 1989). An equilibration process (due to vertical migration) Results in the increasing availability of Fe^{2+} (Bello et al., 2021; Duan et al., 2020; Wilkinson et al., 2000) and HCO_3^- (Smith and Ehrenberg, 1989) shifting the system towards the precipitation of significantly more siderite (Burton et al., 1993).

Widespread carbonate dissolution has been predicted at temperatures above about 110 °C for clastic reservoirs due to the balance between the amount of carbonate available (or its reacting components), its solubility and the equilibrium partial pressure of CO_2 at that depth (Smith and Ehrenberg, 1989). The reservoir temperature of the oilfields in this study is between 42 °C and 90 °C.

5.3. Siderite as a proxy for hydrocarbon migration and implications for hydrocarbon exploration to production

Can the distribution of siderite be a proxy for hydrocarbon migration pathways? To answer this question, we consider the migration history of the hydrocarbons and the distribution of siderite. Analysis of the Bittern field via well cores and reports suggests a significant portion of vertical migration from the Jurassic source rocks to this shallower Palaeogene reservoirs. The drill cuttings together with the resistivity log of the well to the east unlike the other sections of the oilfield revealed significant hydrocarbon shows at stratigraphic boundaries along the well section (Fig. 12). The observed brittleness of these cuttings may be related to salt tectonism and/or the Tertiary rift/inversion related fractures that have provided pathways for hydrocarbon migration to the overlying Forties reservoir. 2-D petroleum systems modelling also supports this interpretation, with evidence of hydrocarbon migration vertically into the area (Badejo et al., 2021a). Synthesizing all these data suggest that vertical migration dominates the east of the field, with lateral migration in the west (Fig. 13). The magnetic data together with the XRD data shows that Bittern oilfield is siderite-rich with its quantity diminishing to the west of the field. We can conclude here that a relationship exists between lateral/vertical hydrocarbon migration and siderite distribution.

The Catcher field comprises both Tay and Cromarty sandstone, juxtaposed against each other as a result of the NW-SE Tertiary fault system (Roberts et al., 2017). The Jurassic source rock in the vicinity of the Catcher field is immature (Isaksen, 2004; Kubala et al., 2003) and the supply of hydrocarbon must have occurred from the deeper basin to the east of the field (Robertson et al., 2013). The Tertiary faulting eventand subsequent sand remobilization that occurred resulted in the oilfield having a Cromarty crest (Gibson et al., 2020). Therefore, both the Cromarty and the Tay section of Catcher field must have been filled with hydrocarbon via lateral migration (Fig. 13). Robertson et al. (2013)

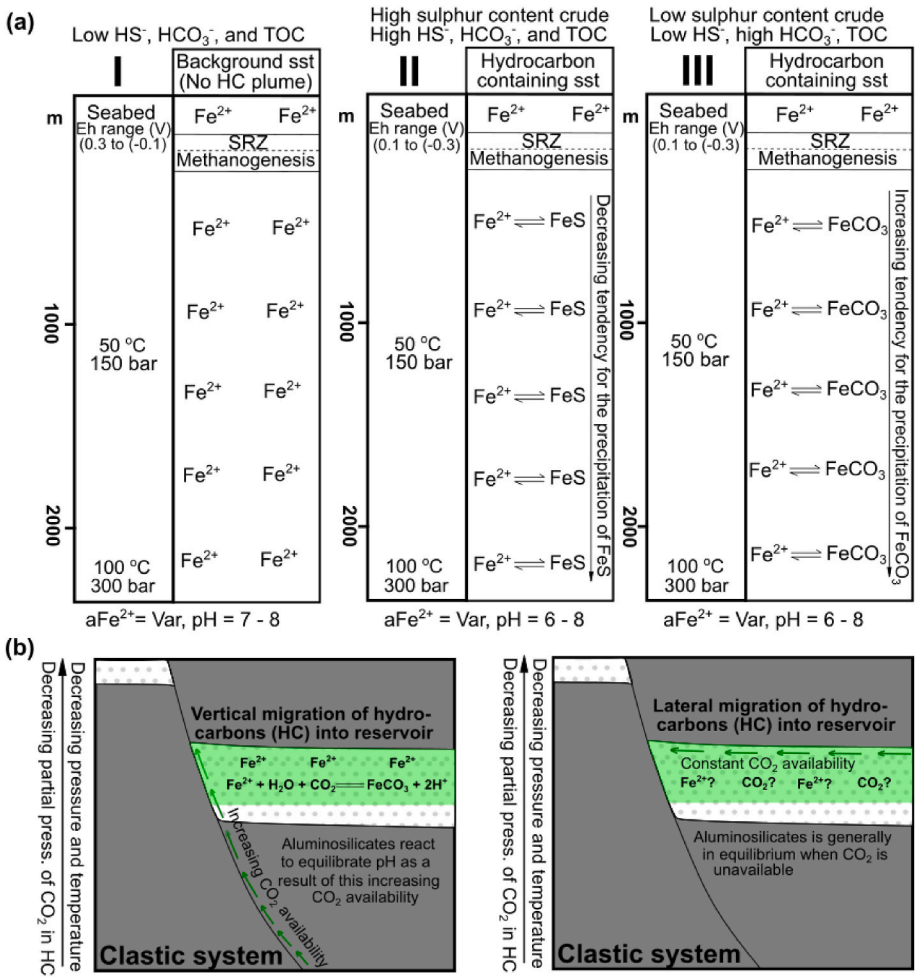

Fig. 11. a) A simplified conceptual model of the most likely magnetic minerals to precipitate in a clastic environment (I) devoid of hydrocarbon (background environment) (II) containing high sulphur content crude (III) containing low sulphur content crude. Fe^{2+} stands for pore water iron, pre-existing magnetic minerals and/or other iron rich minerals. The values of pH, E_h, aFe^{2+}, aHS^{-}, $aHCO_3^{-}$ are obtained from study area and/or experimental data from previous studies (Burton et al., 1993; Hess, 1986; Kuwabara et al., 1999; Miller et al., 2017; Oni et al., 2015; Railsback, 2006) b) Schematic highlighting the difference in siderite precipitation potential for petroleum reservoirs filled via vertical migration versus lateral migration. An increase in available CO_2 and Fe^{2+} is expected in the fields filled via vertical migration relative to fields filled via lateral migration, assuming a low sulphur hydrocarbon system and the presence of iron rich minerals as Fe^{2+} source. HC and Var stand for hydrocarbons and variable respectively.

showed that the Cromarty sandstone is the most likely lateral carrier. The magnetic data (Fig. 7) and XRD data (Table 4) indicate an absence of siderite in the sandstones of this oilfield. From all the data available, we conclude again that a relationship exists between siderite and migration direction i.e., Catcher field was filled laterally and is siderite poor.

The oil pay-zone for the Bonneville and Carnaby oilfields is the Tay sandstone. The Tay sandstone is thin and discontinuous within the CAD region with significant evidence of post-depositional sand remobilization/injection (Badejo, 2019; Gibson et al., 2020; Robertson et al., 2013). The sands are thickest where significant accommodation existed during sediment deposition, e.g., the hanging wall of active Tertiary faults (Fig. 13). Geochemical analysis strongly suggests an east-west fill-spill-chain system during hydrocarbon filling (Forsythe et al., 2017a, 2017b; Gibson et al., 2020). Due to the discontinuous nature of the Tay sandstone, this fill-spill chain into Bonneville and Carnaby likely included faults, fractures and/or small scale injectites (Fig. 13). The lack of a clear present-day pressure communication amongst these fields as suggested by the positions of their oil-water contacts supports this idea (Gibson et al., 2020). Given these complexities, the exact hydrocarbon migration pathway into Bonneville and Carnaby is uncertain; however, the geometry and nature of the fill-spill system (Fig. 13), the nature and the distribution of the reservoir sands and the injectite complex (Gibson et al., 2020) suggest that a significant component of vertical migration has occurred. We have found in this study that these sandstones contain a significant amount of siderite (Fig. 5 and Table 4). From all the data available, we conclude that hydrocarbon migration into Bonneville and Carnaby fields involved significant vertical migration and the sands of these fields are siderite rich.

The combination of all the data we have suggests that the presence and distribution of siderite in hydrocarbon reservoirs can act as a proxy for hydrocarbon migration. The mechanism that promotes the precipitation of siderite as described here together with the data obtained from magnetic experiments support this as the preferred interpretation.

5.4. *Does hydrocarbon biodegradation contribute to siderite formation?*

In hydrocarbon reservoirs with low concentrations of sulphur and at temperatures <80 °C, biodegradation of hydrocarbon may occur and CO_2 produced (Head et al., 2003; Jones et al., 2008). This increases the HCO_3^{-} availability in the system. Therefore, does biodegradation promote an environment favourable for the precipitation of siderite? There is little evidence for this from the literature (e.g Badejo et al., 2021b; Jones et al., 2008). The effect of biodegradation on other factors necessary for the precipitation of siderite must therefore be considered. A few parameters to consider would include the effect of biodegradation on the reactions of the aluminosilicates in sandstones and hence its balancing effect on the pH, the availability of Fe^{2+} for chemical reaction under this condition, its effect on the kinetics of the processes, other products of biodegradation and their effect on the system etc. Biodegradation has been shown to alter the minerology (Ehrenberg and Jakobsen, 2001), formation fluids constituents and acidity (Meredith et al., 2000) in petroleum reservoirs.

The present-day temperature of the Bittern field averages at about 90 °C. Geochemical data from well reports on the Bittern field indicate that the oil here is not biodegraded. However, it contains significant levels of siderite, suggesting a thermogenic source of CO_2. The Catcher

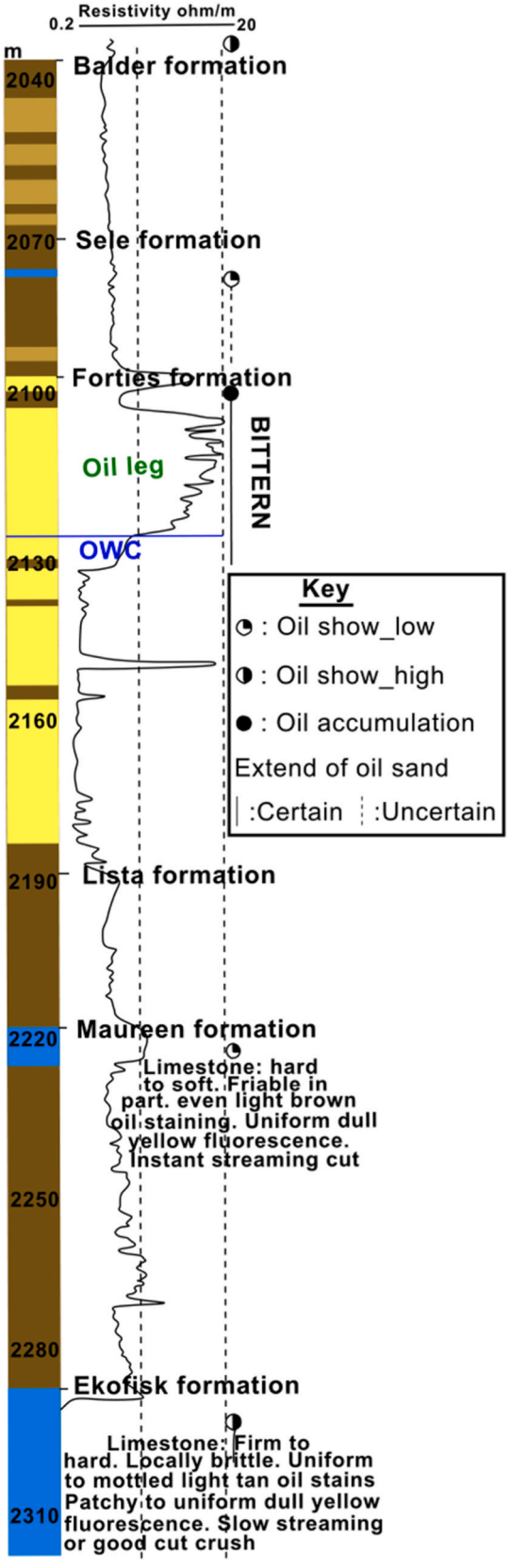

Fig. 12. A section of the composite core from the Bittern well; 29/1a-7 located at the eastern section of the field highlighting hydrocarbon staining along the well section in the Forties, Maureen and Ekofisk formation. The cuttings samples retrieved during drilling showed the friable nature of some of rock section that is likely due to fracturing as a result of salt movement and Tertiary faulting of the West Central Shelf (WCS) etc within that region.

field is classified as slightly biodegraded and has increasing CO_2 in the vicinity of the oil-water contact (Gibson et al., 2020). However, the data from this field suggests negligible levels of siderite (Fig. 6 and Table 4).

The Bonneville and Carnaby fields are both moderately biodegraded reservoirs (Forsythe et al., 2017a, 2017b), with significant biodegradation having occurred downdip along the fill-spill chain during migration (Gibson et al., 2020). These fields also have high levels of siderite (Fig. 9 and Table 4). Is the siderite formed due to reactants formed via a biogenic or thermogenic process? The stable isotope data suggests that the siderite likely formed from HCO_3^-/CO_2 derived from variable sources, but its main source is of thermogenic origin (Fig. 9). Values of $\delta^{13}C$ less than 2‰ (VPDB) for CO_2 contained in petroleum reservoir fluids are generally interpreted to have been derived via a thermogenic or inorganic process (Milkov, 2018). This supports a hydrocarbon migration source and hence our conclusion. Stable isotope analysis were also carried on samples from the Bittern oilfield, however, the Results were inconclusive as the data plotted in a region of uncertainty that supports both a thermogenic (Milkov, 2018; Pankina, 1979) and a biogenic (Milkov, 2018) origin.

6. Conclusions

Through detailed magnetic studies of reservoir sandstones for four oilfields in the UK Central North Sea, we have identified:

i) The presence of siderite, iron sulphide, magnetite, hematite and Ti-rich iron oxides in these hydrocarbon bearing sandstones, unlike nearby dry well sandstones (background) where only magnetite, hematite and Ti-rich iron oxides were identified. Siderite is interpreted to form as a result of vertical hydrocarbon migration into these reservoir sandstones.
ii) Due to the precipitated siderite in these oilfield sandstones, a significantly higher, but variable, paramagnetic response compared to the background sands is observed. High-field susceptibility χ_{hf} and the magnetic susceptibility χ revealed a good correlation with amount of siderite, and hence presents as a reliable proxy for hydrocarbon migration.
iii) A relationship has been observed between the presence of siderite in an oilfield and hydrocarbon migration direction. The oilfield, i.e., Catcher that filled via laterally migration was siderite poor whilst the oilfields, i.e., Bittern, Bonneville and Carnaby, filled via vertical migration were siderite rich.

The relationship between migration direction and siderite formation is as a result of the interplay between the changes in equilibrium partial pressures of CO_2 with depth, the ubiquitous presence of CO_2 in migrating hydrocarbons and the geochemical requirements for the precipitation of siderite. Biodegradation of hydrocarbon is an important parameter to consider, but it is unlikely that this will have an obscuring effect on siderite precipitation due to hydrocarbon migration.

CRediT authorship contribution

Abdulkarim, Maryam Ahmed: Conceptualization, Data curation, Experimentation, Formal analysis, Investigation, Methodology, Validation, Writing – original draft & editing. **Adrian R. Muxworthy:** Conceptualization, Supervision, Writing – review & editing. **Alastair Fraser:** Conceptualization, Supervision, Writing – review & editing. **Martin Neumaier:** Investigation, Supervision. **Pengxiang Hu:** Experimentation, Writing – review & editing. **Alison Cowan** Experimentation.

Data availability

All the data used in this study would be available from June 2021 in the appendix of PhD thesis of Abdulkarim (2021) at www.spiral.imperial.ac.uk.

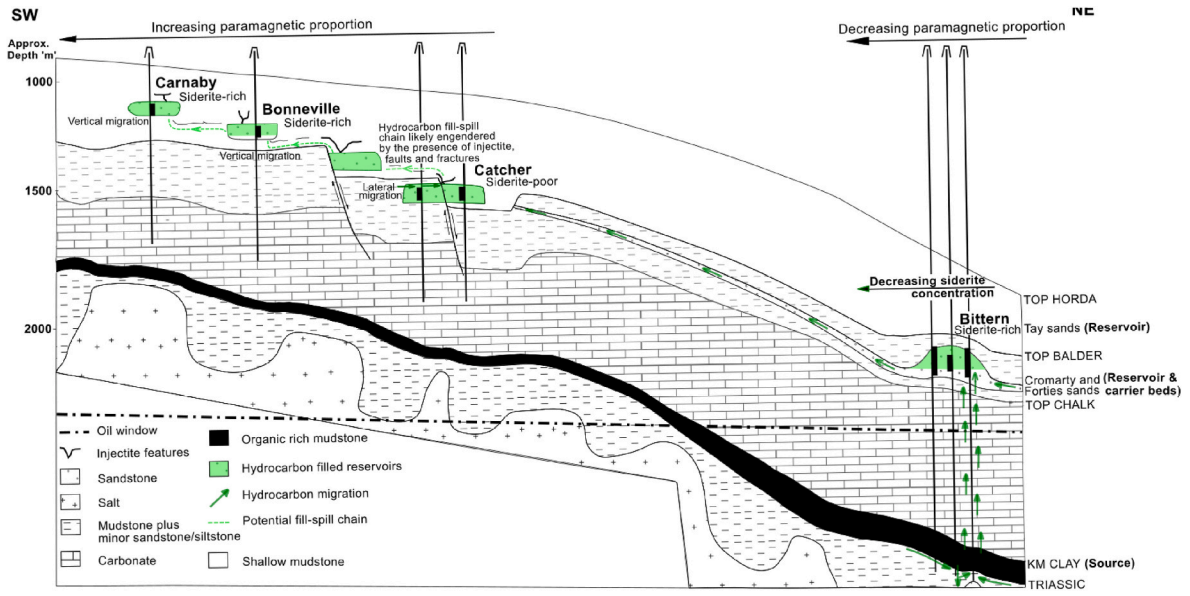

Fig. 13. A schematic of a south west- north east cross-section through the Bittern and CAD fields showing the most likely migration pathways of hydrocarbon into these oilfields. The variation in paramagnetic proportion and the distribution of siderite is also highlighted. The regions dominated by vertical migration (i.e Bittern, Carnaby and Bonneville fields) are generally siderite rich. The region charged via lateral migration (i.e. the Catcher field) are siderite poor. Approximate horizontal extent of 2D section is 40 km.

Declaration of competing interest

The authors declare that they have no known competing financial interests or personal relationships that could have appeared to influence the work reported in this paper.

Acknowledgement

This work was funded by Petroleum Technology Development Fund (PTDF) Nigeria, and a Visiting Fellowship to the Institute of Rock Magnetism (IRM), University of Minnesota. The IRM is funded by the Instruments and Facilities program of the Earth Sciences Division of the National Science Foundation, and by the University of Minnesota. We thank the UKRI and the BGS for the core samples.

References

Abubakar, R., Muxworthy, A.R., Fraser, A., Sephton, M.A., Watson, J.S., Heslop, D., Paterson, G.A., Southern, P., 2020. Mapping hydrocarbon charge-points in the Wessex Basin using seismic, geochemistry and mineral magnetics. Mar. Petrol. Geol. 111, 510–528. https://doi.org/10.1016/j.marpetgeo.2019.08.042.

Ahmadi, Z., Sawyers, M., Kenyon-Roberts, S., Stanworth, C., Kugler, K., Kristensen, J., Fugelli, E., 2003. Paleocene. In: Evans, D., Graham, C., Armour, A., Bathurst, P. (Eds.), The Millennium Atlas: Petroleum Geology of the Central and Northern North Sea. The Geological Society of London. https://doi.org/10.1017/S0016756803218124.

Badejo, S.A., 2019. Using Magnetic Techniques to Calibrate Lateral Hydrocarbon Migration in Basin Modelling: A Case Study from the Lower Tertiary, UK Central North Sea. Imperial College. PhD Thesis.

Badejo, S.A., Fraser, A.J., Neumaier, M., Muxworthy, A.R., Perkins, J.R., 2021a. 3D petroleum systems modelling as an exploration tool in mature basins: a study from the Central North SeaUK. Mar. Petrol. Geol. 133, 105271. https://doi.org/10.1016/j.marpetgeo.2021.105271.

Badejo, S.A., Muxworthy, A., Fraser, A., Stevenson, G., Zhao, X., Jackson, M., 2021b. Identification of Magnetic Enhancement at Hydrocarbon/water Contacts 10, pp. 1973–1991. https://doi.org/10.1306/07062019207.

Badejo, S.A., Muxworthy, A.R., Fraser, A., Neumaier, M., Perkins, J.R., Stevenson, G.R., Davey, R., 2021c. Using magnetic techniques to calibrate hydrocarbon migration in petroleum systems modelling: a case study from the Lower Tertiary, UK Central North Sea. Geophys. J. Int. 227, 617–631. https://doi.org/10.1093/gji/ggab236.

Bello, A.M., Jones, S., Gluyas, J., Acikalin, S., Cartigny, M., 2021. Role played by clay content in controlling reservoir quality of submarine fan system, Forties Sandstone Member, Central Graben, North Sea. Mar. Petrol. Geol. 128, 105058. https://doi.org/10.1016/j.marpetgeo.2021.105058.

Burton, E.A., Machel, H.G., Qi, J., 1993. Thermodynamic constraints on anomalous magnetization in shallow and deep hydrocarbon seepage environments. In: SEPM Special Publication. SEPM Society for Sedimentary Geology, pp. 193–207. https://doi.org/10.2110/pec.93.49.

Campbell, Michael D., Campbell, M David, 2018. Paleoenvironmental implications of selected siderite zones in the upper Atoka formation, Arkoma basin, Oklahoma-Arkansas: a look back and current views on siderite genesis in a sedimentary environment. Int. J. Earth Sci. Geol. 1, 6–40. https://doi.org/10.18689/ijeg-1000103.

Costanzo-Alvarez, V., Aldana, M., Díaz, M., Bayona, G., Ayala, C., 2006. Hydrocarbon-induced magnetic contrasts in some Venezuelan and Colombian oil wells. Earth Planets Space 58, 1401–1410. https://doi.org/10.1186/BF03352636.

Doebelin, N., Kleeberg, R., 2015. Profex : a graphical user interface for the Rietveld refinement program BGMN. J. Appl. Crystallogr. 48, 1573–1580. https://doi.org/10.1107/S1600576715014685.

Duan, W., Li, C., Luo, C., Chen, J., Huang, X., Yan, Z., 2020. Formation of an anomalously high-porosity zone of a very fine-grained deep clastic reservoir in the Qiongdongnan Basin, South China Sea. Geol. J. 55, 8244–8263. https://doi.org/10.1002/gj.3938.

Dyar, M.D., Agresti, D.G., Schaefer, M.W., Grant, C.A., Sklute, E.C., 2006. Mössbauer spectroscopy of Earth and planetary materials. Annu. Rev. Earth Planet Sci. 34, 83–125. https://doi.org/10.1146/annurev.earth.34.031405.125049.

Ehrenberg, S.N., Jakobsen, K.G., 2001. Plagioclase dissolution related to biodegradation of oil in brent group sandstones (middle Jurassic) of Gullfaks field, Northern North sea. Sedimentology 48, 703–721. https://doi.org/10.1046/j.1365-3091.2001.00387.x.

Eldrett, J., Tripsanas, E., Davis, C., McKie, T., Vieira, M., Osterloff, P., Sandison, T., 2015. Sedimentological evolution of Sele formation deep-marine depositional systems of the Central North sea. Geol. Soc. Spec. Publ. 403, 63–98. https://doi.org/10.1144/SP403.9.

Emmerton, S., Muxworthy, A.R., Sephton, M.A., Aldana, M., Costanzo-Alvarez, V., Bayona, G., Williams, W., 2013. Correlating biodegradation to magnetization in oil bearing sedimentary rocks. Geochem. Cosmochim. Acta 112, 146–165. https://doi.org/10.1016/j.gca.2013.03.008.

Emmerton, S.A., 2013. Investigating the Relationship between Magnetisation and Oil Geochemistry. Imperial College. PhD Thesis.

Forsythe, J.C., De Santo, I., Martin, R., Tyndall, R., Arman, K., Pye, J., O'Donnell, M., Kenyon-Roberts, S., Nelson, R.K., Reddy, C.M., Pomerantz, A.E., Canas, J.A., Zuo, J. Y., Peters, K.E., Mullins, O.C., 2017a. Reservoir implications of a spill-fill sequence of reservoir charge coupled with viscosity and asphaltene gradients from a combination of water washing and biodegradation. In: SPE Annual Technical Conference and Exhibition. Society of Petroleum Engineers. https://doi.org/10.2118/187044-MS.

Forsythe, Jerimiah C., Martin, R., De Santo, I., Tyndall, R., Arman, K., Pye, J., De Nicolais, N., Nelson, R.K., Pomerantz, A.E., Kenyon-Roberts, S., Zuo, J.Y., Betancourt, S.S., Reddy, C., Peters, K.E., Mullins, O.C., 2017b. Integrating comprehensive two-dimensional gas chromatography and downhole fluid analysis to validate a spill-fill sequence of reservoirs with variations of biodegradation, water washing and thermal maturity. Fuel 191, 538–554. https://doi.org/10.1016/j.fuel.2016.11.081.

Fraser, S.I., Robinson, A.M., Johnson, H.D., Underhill, J.R., Kadolsky, D.G.A., Connell, R., Johannessen, P., R, R., 2003. Upper Jurassic. In: Evans, M.E., Michael, E., Graham, C., Armour, A., Bathurst, P. (Eds.), The Millennium Atlas: Petroleum Geology of the Central and Northern North Sea. The Geological Society of London, pp. 157–189. https://doi.org/10.1017/S0016756803218124.

Gibson, M., Riley, D., Kenyon-Roberts, S., Opata, J., Beck, A., Nguyen, C., Martin, T., 2020. The catcher, varadero and burgman fields, block 28/9a, UK North Sea. Geol. Soc. Lond. Mem 52, 399–412. https://doi.org/10.1144/m52-2019-24.

Head, I.M., Jones, D.M., Larter, S.R., 2003. Biological activity in the deep subsurface and the origin of heavy oil. Nature 426, 344–352. https://doi.org/10.1038/nature02134.

Hess, R., 1986. Diagenesis #11. Early diagenetic pore water/sediment interaction: modern offshore basins. Geosci. Can. 13, 165–196.

Hounslow, M.W., Maher, B.A., Thistlewood, L., 1995. Magnetic mineralogy of sandstones from the Lunde formation (late Triassic), Northern North sea, UK: origin of the palaeomagnetic signal. Geol. Soc. Spec. Publ. 98, 119–147. https://doi.org/10.1144/GSL.SP.1995.098.01.07.

Huggett, J.M., 1996. Aluminosilicate diagenesis in Tertiary sandstone-mudrock sequence from the Central North sea, UK. Clay Miner. 31, 523–536.

Hutcheon, I., Abercrombie, H., 1990. Carbon dioxide in clastic rocks and silicate hydrolysis. Geology 18, 541. https://doi.org/10.1130/0091-7613(1990)018<0541:CDICRA>2.3.CO;2.

Isaksen, G.H., 2004. Central North Sea hydrocarbon systems: generation, migration, entrapment, and thermal degradation of oil and gas. Am. Asoc. Pet. Geol. 1545–1572. https://doi.org/10.1002/clc.4960050609.

Jacobs, I.S., 1963. Metamagnetism of siderite ($FeCO_3$). J. Appl. Phys. 34, 1106–1107.

Jones, D.M., Head, I.M., Gray, N.D., Adams, J.J., Rowan, A.K., Aitken, C.M., Bennett, B., Huang, H., Brown, A., Bowler, B.F.J., Oldenburg, T., Erdmann, M., Larter, S.R., 2008. Crude-oil biodegradation via methanogenesis in subsurface petroleum reservoirs. Nature 451, 176–180. https://doi.org/10.1038/nature06484.

Jones, E., Jones, R., Ebdon, C., Ewen, D., Milner, P., Plunkett, J., Hudson, G., Slater, P., 2003. Eocene. In: Evans, D., Graham, C., Armour, A., Bathurst, P. (Eds.), The Millennium Atlas: Petroleum Geology of the Central and Northern North Sea. The Geological Society of London, London, pp. 261–277.

Kubala, M., Bastow, M., Thompson, S., Scotchman, I., Oygard, K., 2003. Geothermal regime, petroleum generation and migration. In: Evans, D., Graham, C., Armour, A., Bathurst, P. (Eds.), The Millennium Atlas: Petroleum Geology of the Central and Northern North Sea. The Geological Society of London. https://doi.org/10.1017/S0016756803218124.

Kuwabara, J.S., Van Geen, A., McCorkle, D.C., Bernhard, J.M., 1999. Dissolved sulfide distributions in the water column and sediment pore waters of the Santa Barbara Basin. Geochem. Cosmochim. Acta 63, 2199–2209. https://doi.org/10.1016/S0016-7037(99)00084-8.

Larrasoaña, J.C., Roberts, A.P., Musgrave, R.J., Gràcia, E., Piñero, E., Vega, M., Martínez-Ruiz, F., 2007. Diagenetic formation of greigite and pyrrhotite in gas hydrate marine sedimentary systems. Earth Planet Sci. Lett. 261, 350–366. https://doi.org/10.1016/j.epsl.2007.06.032.

Lin, C.Y., Turchyn, A.V., Krylov, A., Antler, G., 2020. The microbially driven formation of siderite in salt marsh sediments. Geobiology 18, 207–224. https://doi.org/10.1111/gbi.12371.

Liu, M., Chen, Z., Chen, Q., 1997. The role of organic matter in the formation of siderite from Xuanlong Area, Hebei Province. Chin. J. Geochem. 16.

Macaulay, C.I., Haszeldine, R.S., Fallick, A.E., 1993. Distribution, chemistry, isotopic composition and origin of diagenetic carbonates: magnus Sandstone, North Sea. J. Sediment. Petrol. 63, 33–43. https://doi.org/10.1306/D4267A82-2B26-11D7-8648000102C1865D.

Machel, H.G., 1995. Magnetic mineral assemblages and magnetic contrasts in diagenetic environments — with implications for studies of palaeomagnetism, hydrocarbon migration and exploration. Geol. Soc. Lond. Spec. Publ. 98, 9–29. https://doi.org/10.1144/gsl.sp.1995.098.01.02.

Machel, H.G., Burton, A., 1991. Chemical and microbial processes causing anomalous magnetization in environments affected by hydrocarbon seepage. Geophysics 56, 598–605. https://doi.org/10.1038/nsmb.2400.

Mccormick, D., Leishman, M., 2004. The Bittern Field: Topographic Control of an Eocene Aged "'Channel- Fill"' Turbidite Reservoir in the U.K. Central North Sea*. North 20,016, pp. 1–6.

Meredith, W., Kelland, S.J., Jones, D.M., 2000. Influence of biodegradation on crude oil acidity and carboxylic acid composition. Org. Geochem. 31, 1059–1073. https://doi.org/10.1016/S0146-6380(00)00136-4.

Milkov, A.V., 2018. Secondary microbial gas. Hydrocarb. Oils lipids divers. Orig. Chem. Fate 1–10. https://doi.org/10.1007/978-3-319-54529-5_22-1.

Miller, C.M., Dickens, G.R., Jakobsson, M., Johansson, C., Koshurnikov, A., O'Regan, M., Muschitiello, F., Stranne, C., 2017. Pore water geochemistry along continental slopes north of the East Siberian Sea: inference of low methane concentrations. Biogeosciences 14, 2929–2953. https://doi.org/10.5194/bg-14-2929-2017.

Morin, F.J., 1950. Magnetic susceptibility of α-Fe2O3 and α-Fe2O3 with added titanium. Phys. Rev. 78, 819–820. https://doi.org/10.1103/PhysRev.78.819.2.

Moskowitz, B.M., Jackson, M., Kissel, C., 1998. Low-temperature magnetic behavior of titanomagnetites. Earth Planet Sci. Lett. 157, 141–149. https://doi.org/10.1016/S0012-821X(98)00033-8.

Mudge, D.C., 2015. Regional controls on lower Tertiary sandstone distribution in the north sea and NE Atlantic margin basins. Geol. Soc. Spec. Publ. 403, 17–42. https://doi.org/10.1144/SP403.5.

Muxworthy, A.R., McClelland, E., 2000. Review of the low-temperature magnetic properties of magnetite from a rock magnetic perspective. Geophys. J. Int. 140, 101–114. https://doi.org/10.1046/j.1365-246x.2000.00999.x.

Oni, O., Miyatake, T., Kasten, S., Richter-Heitmann, T., Fischer, D., Wagenknecht, L., Kulkarni, A., Blumers, M., Shylin, S.I., Ksenofontov, V., Costa, B.F.O., Klingelhöfer, G., Friedrich, M.W., 2015. Distinct microbial populations are tightly linked to the profile of dissolved iron in the methanic sediments of the Helgoland mud area, North Sea. Front. Microbiol. 6 https://doi.org/10.3389/fmicb.2015.00365.

Pan, Y., Zhu, R., Banerjee, S.K., Gill, J., Williams, Q., 2000. Rock magnetic properties related to thermal treatment of siderite: behavior and interpretation. J. Geophys. Res. Solid Earth 105, 783–794. https://doi.org/10.1029/1999jb900358.

Pankina, R.G., 1979. Origin of CO2 in petroleum gases (from the isotopic composition of carbon). Int. Geol. Rev. 21, 535–539. https://doi.org/10.1080/00206818209467089.

Railsback, B.L., 2006. Some Fundamentals of Mineralogy and Geochemistry. Department of Geology, University of Georgia Athens, Georgia 30602-2501 U.SA.

Ritchie, A.L., Hodzic, M., Brain, J., Coogan, S., Khan, S., Mcclean, S., Okubanjo, L., Cowie, D., 2011. Bittern Further Developed through Integration (Devex).

Roberts, A.P., 2015. Magnetic mineral diagenesis. Earth Sci. Rev. 151, 1–47. https://doi.org/10.1016/j.earscirev.2015.09.010.

Roberts, S.K., Riley, D., Gibson, M., Nguyen, C., Martin, T., Beck, A., Bower, M., Perna, F., Bisain, A., Hui, X.C., Steele, J.W., 2017. Say no to pilot-holes and sidetracks - mapping complex injectite sand reservoirs while landing and from inside - case studies from the catcher development. In: SPE Offshore Europe Conference & Exhibition. Society of Petroleum Engineers. https://doi.org/10.2118/186136-MS.

Robertson, J., Goulty, N.R., Swarbrick, R.E., 2013. Overpressure distributions in Palaeogene reservoirs of the UK Central North Sea and implications for lateral and vertical fluid flow. Petrol. Geosci. 19, 223–236. https://doi.org/10.1144/petgeo2012-060.

Rochette, P., Fillion, G., Mattéi, J.L., Dekkers, M.J., 1990. Magnetic transition at 30-34 Kelvin in pyrrhotite: insight into a widespread occurrence of this mineral in rocks. Earth Planet Sci. Lett. 98, 319–328. https://doi.org/10.1016/0012-821X(90)90034-U.

Rossi, C., Marfil, R., Ramseyer, K., Permanyer, A., 2001. Facies-related diagenesis and multiphase siderite cementation and dissolution in the reservoir sandstones of the Khatatba formation, Egypt's western Desert. J. Sediment. Res. 71, 459–472. https://doi.org/10.1306/2dc40955-0e47-11d7-8643000102c1865d.

Smith, J.T., Ehrenberg, S.N., 1989. Correlation of carbon dioxide abundance with temperature in clastic hydrocarbon reservoirs: relationship to inorganic chemical equilibrium. Mar. Petrol. Geol. 6, 129–135. https://doi.org/10.1016/0264-8172(89)90016-0.

Sprain, C.J., Feinberg, J.M., Renne, P.R., Jackson, M., 2016. Importance of titanohematite in detrital remanent magnetizations of strata spanning the Cretaceous-Paleogene boundary, Hell Creek region, Montana Courtney. Geochem. Geophys. Geosyst. 17, 1312–1338. https://doi.org/10.1002/2015GC006205. Received.

Stevens, J.G., Khasanov, A.M., Miller, J.W., Pollak, H., Li, Z., 1998. Mössbauer Mineral Handbook, 3rd Ediito. Mossbauer Effect Data Center, Asheville.

Stewart, S.A., 1996. Tertiary extensional fault systems on the western margin of the North Sea Basin. Petrol. Geosci. 2, 167–176. https://doi.org/10.1144/petgeo.2.2.167.

Ufer, K., Roth, G., Kleeberg, R., Stanjek, H., Dohrmann, R., Bergmann, J., 2004. Description of X-ray powder pattern of turbostratically disordered layer structures with a Rietveld compatible approach. Z. für Kristallogr. - Cryst. Mater. 219, 519–527. https://doi.org/10.1524/zkri.219.9.519.44039.

Verwey, E.J.W., 1939. Electronic conduction of magnetite (Fe_3O_4) and its transition point at low temperatures. Nature 144, 327–328. https://doi.org/10.1038/144327b0.

Wilkinson, M., Haszeldine, R.S., Fallick, A.E., 2006. Jurassic and Cretaceous clays of the northern and central North Sea hydrocarbon reservoirs reviewed. Clay Miner. 41, 151–186. https://doi.org/10.1180/0009855064110197.

Wilkinson, M., Haszeldine, R.S., Fallick, A.E., Osborne, M.J., 2000. Siderite zonation within the Brent Group: microbial influence or aquifer flow? Clay Miner. 35, 107–117. https://doi.org/10.1180/000985500546512.

Zarghami, S., Boukadi, F., Al-Wahaibi, Y., 2017. Diffusion of carbon dioxide in formation water as a result of CO2 enhanced oil recovery and CO_2 sequestration. J. Pet. Explor. Prod. Technol. 7, 161–168. https://doi.org/10.1007/s13202-016-0261-7.

Zuo, L., Zhang, C., Falta, R.W., Benson, S.M., 2013. Micromodel investigations of CO_2 exsolution from carbonated water in sedimentary rocks. Adv. Water Resour. 53, 188–197. https://doi.org/10.1016/j.advwatres.2012.11.004.